Molecular Biology of the Cell
Vol. 21, 73–86, January 1, 2010

Na^+/H^+ Exchanger Regulatory Factor 1 Overexpression-dependent Increase of Cytoskeleton Organization Is Fundamental in the Rescue of F508del Cystic Fibrosis Transmembrane Conductance Regulator in Human Airway CFBE41o- Cells

Maria Favia,*† Lorenzo Guerra,*† Teresa Fanelli,* Rosa Angela Cardone,* Stefania Monterisi,* Francesca Di Sole,‡ Stefano Castellani,§ Mingmin Chen,‖ Ursula Seidler,‖ Stephan Joel Reshkin,* Massimo Conese,§ and Valeria Casavola*

*Department of General and Environmental Physiology, University of Bari, Bari 70126, Italy; ‡Department of Internal Medicine and Pak Center of Mineral Metabolism and Clinical Research, University of Texas Southwestern Medical Center, Dallas, TX 75390-8885; §Department of Biomedical Sciences, University of Foggia, 71100 Foggia, Italy; and ‖Department of Gastroenterology, Hannover Medical School, Hannover 30625, Germany

Submitted March 5, 2009; Revised October 7, 2009; Accepted October 28, 2009
Monitoring Editor: Keith E. Mostov

We have demonstrated that Na^+/H^+ exchanger regulatory factor 1 (NHERF1) overexpression in CFBE41o- cells induces a significant redistribution of F508del cystic fibrosis transmembrane conductance regulator (CFTR) from the cytoplasm to the apical membrane and rescues CFTR-dependent chloride secretion. Here, we observe that CFBE41o- monolayers displayed substantial disassembly of actin filaments and that overexpression of wild-type (wt) NHERF1 but not NHERF1-Δ Ezrin-Radixin-Moesin (ERM) increased F-actin assembly and organization. Furthermore, the dominant-negative band Four-point one, Ezrin, Radixin, Moesin homology (FERM) domain of ezrin reversed the wt NHERF1 overexpression-induced increase in both F-actin and CFTR-dependent chloride secretion. wt NHERF1 overexpression enhanced the interaction between NHERF1 and both CFTR and ezrin and between ezrin and actin and the overexpression of wt NHERF1, but not NHERF1-ΔERM, also increased the phosphorylation of ezrin in the apical region of the cell monolayers. Furthermore, wt NHERF1 increased RhoA activity and transfection of constitutively active RhoA in CFBE41o- cells was sufficient to redistribute phospho-ezrin to the membrane fraction and rescue both the F-actin content and the CFTR-dependent chloride efflux. Rho kinase (ROCK) inhibition, in contrast, reversed the wt NHERF1 overexpression-induced increase of membrane phospho-ezrin, F-actin content, and CFTR-dependent secretion. We conclude that NHERF1 overexpression in CFBE41o- rescues CFTR-dependent chloride secretion by forming the multiprotein complex RhoA-ROCK-ezrin-actin that, via actin cytoskeleton reorganization, tethers F508del CFTR to the cytoskeleton stabilizing it on the apical membrane.

INTRODUCTION

One of the key membrane proteins regulating overall fluid movement is the cystic fibrosis transmembrane conductance regulator (CFTR). Besides regulating other ion transporters, CFTR is itself a cAMP-activated chloride channel expressed in luminal membranes of secretory and reabsorptive epithelia (Sheppard and Welsh, 1999). In normal cells, newly synthesized wt CFTR protein, after passing the endoplasmic reticulum (ER) quality control, is exported from the Golgi to the apical membrane as fully glycosylated CFTR. Once arrived at the plasma membrane, CFTR binds to associate proteins, which may finely regulate its stability and activity. Indeed, the carboxy-terminal postsynaptic density 95/disc-large/zona occludens (PDZ) binding motif of CFTR has been found to interact with many PDZ domain-containing proteins, such as Na^+/H^+ exchanger regulatory factor 1 (NHERF1), CFTR Associated Ligand, and CFTR Associated Protein 70, and the physiological significance of these adaptor proteins in the regulation of CFTR activity has been verified in several studies (Hall *et al*., 1998; Wang *et al*., 2000; Raghuram *et al*., 2001; Cheng *et al*., 2002; Benharouga *et al*., 2003; Li and Naren, 2005). In particular NHERF1, in addition

This article was published online ahead of print in *MBC in Press* (http://www.molbiolcell.org/cgi/doi/10.1091/mbc.E09–03–0185) on November 4, 2009.

† These authors contributed equally to this work.

Address correspondence to: Valeria Casavola (casavola@biologia.uniba.it).

Abbreviations used: ER, endoplasmic reticulum; ERM, Ezrin-Radixin-Moesin; FERM, band Four-point one, Ezrin, Radixin, Moesin homology domain; GFP, green fluorescent protein; GST, glutathione transferase; NHERF1, Na^+/H^+ exchanger regulatory factor 1; N-WASP, neural Wiskott-Aldrich syndrome protein; PDZ, postsynaptic density 95/disc-large/zona occludens; RBD, Rho-binding domain; ROCK, Rho kinase; wt, wild type.

to interacting directly with CFTR, permits a spatial grouping and the physical association of different key signal transduction components such as phospholipase C, Yes-Associated Protein 65, and Receptor for Activated C-Kinase 1 with CFTR (for review, see Guggino and Stanton, 2006), and in this way, allows the fine regulation of CFTR activity. Moreover, by its C-terminal domain NHERF1 binds the protein kinase A (PKA)-anchoring protein ezrin, which modulates the PKA-dependent CFTR activity (Sun *et al*., 2000).

The most common mutation of the *CFTR* gene associated with cystic fibrosis (CF) causes deletion of phenylalanine at residue 508 (F508del CFTR), and this mutation results in the synthesis of an improperly folded CFTR protein that, although being partially functional and responsive to cAMP/PKA regulation, is unable to reach the cell membrane due to retention and/or accelerated degradation in the ER. However, in some CF airway cells a negligible expression of F508del CFTR can be detected at the cell surface due to the fact that ER retention is not complete (Kalin *et al*., 1999; Bronsveld *et al*., 2000). Furthermore, the F508del-mutation reduces its apical membrane half-life (Lukacs *et al*., 1993; Sharma *et al*., 2001) by accelerating its endocytic retrieval from the plasma membrane and its consequent degradation (Swiatecka-Urban *et al*., 2005). Recently, it has been found in the polarized human CF airway epithelial cell line CFBE41o- that NHERF1 depletion causes F508del CFTR, which has been rescued to cell membrane, to be more susceptible to degradation with a consequent reduction of its residence time at the cell surface (Kwon *et al*., 2007).

In line with these observations, we have demonstrated previously that NHERF1 overexpression increases the wild-type (wt) CFTR expression on the apical membrane in human airway cells, 16HBE14o-, and rescues F508del CFTR functional expression in CFBE41o- cells by inducing the redistribution of F508del CFTR from the cytoplasm to the plasma membrane and by increasing the PKA-dependent activation of CFTR-dependent chloride secretion (Guerra *et al*., 2005). This F508del CFTR redistribution could be a consequence of various interacting factors because CFTR membrane expression and activity have been shown to depend on F-actin cytoskeletal organization (Haggie *et al*., 2004; Ganeshan *et al*., 2007; Okiyoneda and Lukacs, 2007), and NHERF1 is known to mediate the association between CFTR and the cytoskeleton via the actin binding protein ezrin (Short *et al*., 1998; Moyer *et al*., 1999).

The aim of this study was to explore the hypothesis that NHERF1 overexpression in CFBE41o- cells may influence F508del CFTR functional expression to the apical membrane via cytoskeleton organization and the formation of multiprotein complex NHERF1-ezrin-actin. We found that NHERF1 overexpression through its linkage with ezrin increases F-actin organization and assembly in CFBE41o- cell monolayers and also positively regulates the activation of RhoA. This up-regulation of RhoA activity, in turn, leads to Rho kinase (ROCK)-mediated ezrin phosphorylation and stabilization in its open, active conformation, which further increases F508del CFTR stability in the apical membrane by tethering it to the actin cytoskeleton.

MATERIALS AND METHODS

Materials

The primary antibodies used for immunocytochemical analysis and Western blots were as follows: monoclonal anti-human ezrin and anti-human NHERF1 (BD Transduction Laboratories, Milan, Italy), monoclonal anti-human CFTR against the C terminus (R&D Systems, Minneapolis, MN), monoclonal anti-CFTR (CF3; Abcam, Cambridge United Kingdom), polyclonal anti-human phospho-Ezrin (Thr567)/Radixin (Thr564)/Moesin (Thr558) and anti-His-Tag (Cell Signaling Technology, Danvers, MA), polyclonal anti-NHERF1 (ABR–Affinity BioReagents, Golden, CO), monoclonal anti-Na^+/K^+-ATPase β-1, clone C4646 (Millipore, Billerica, MA), goat polyclonal anti-70-kDa heat-shock protein (HSP) and monoclonal anti-RhoA (Santa Cruz Biotechnology, Santa Cruz, CA), monoclonal anti-α-actinin (Cytoskeleton, Denver, CO), monoclonal anti-β-actin and anti-hemagglutinin (HA) (Sigma-Aldrich, St. Louis, MO). The appropriate secondary antibodies were purchased from Sigma-Aldrich or Invitrogen (Carlsbad, CA).

Forskolin (FSK), $CFTR_{inh}$-172, hygromycin B, and Y-27632 were purchased from Calbiochem (San Diego, CA). 3-Isobutyl-1-methylxanthine (IBMX), Escort IV, and phalloidin-tetramethylrhodamine B isothiocyanate (TRITC) were purchased from Sigma-Aldrich, and EZ-LinkSulfo-NHS-SS-Biotin and streptavidin agarose resin were purchased from Pierce Chemical (Rockford, IL). *N*-(Ethoxycarbonylmethyl)-6-methoxyquinolinium bromide (MQAE) and Lipofectamine 2000 reagent were purchased from Invitrogen.

Cell Culture

Experiments were performed with two human bronchial epithelial cell lines: the normal 16HBE14o- cells and the CFBE41o- cells homozygous for the F508del allele (F508del/F508del) (a generous gift from Prof. D. Gruenert, University of California–San Francisco, San Francisco, CA). The cells were grown in Eagle's minimal essential medium (MEM) (EuroClone, Milan, Italy) supplemented with 10% fetal bovine serum (Invitrogen), L-glutamine, and penicillin/streptomycin at 37°C under 5% CO_2. They were routinely grown on plastic flasks coated with an extracellular matrix containing fibronectin/vitrogen/bovine serum albumin. The extracellular matrix coating was prepared in the laboratory as follows: 10 μg/ml fibronectin adhesion-promoting peptide (Sigma-Aldrich), 100 μg/ml albumin from bovine serum (Sigma-Aldrich), and 30 μg/ml bovine collagen type I (BD Transduction Laboratories) were dissolved in MEM. The mixture was sterilized by 0.2-μm filter. Each substrate plastic, glass, or permeable support was coated with the mixture for 2 h at 37°C before cell seeding. For chloride efflux experiments, confocal immunofluorescence analysis and internalization assay cells were seeded on 0.4-μm pore size PET filter inserts (Falcon; BD Biosciences Discovery Labware, Bedford, MA) coated with the same extracellular matrix.

Transfection of Cells

At 70–80% confluence, cells were transiently transfected with mouse NHERF1 cDNA constructs, with human ezrin cDNA constructs, or with human RhoA cDNA constructs by using Escort IV reagent according to the manufacturer's protocol, and the experiments were conducted 48 h later. wt NHERF1 and NHERF1-ΔERM encoding NHERF1 truncated of the last 30 amino acids inserted in pcDNA3.1/Hygro+ vector were generously provided by Prof. E. J. Weinman (University of Maryland Hospital, Baltimore, MD). The FERM domain of ezrin, including amino acids 1-308, subcloned in pEGFP-N3, was generously provided by Prof. S. Cotecchia (Department of General and Environmental Physiology, University of Bari, Bari, Italy). The dominant-negative RhoA, RhoA-N19 3xHA tagged (N terminus), inserted into pcDNA3.1/Hygro+ vector, was provided by Missouri S&T cDNA Resource Center (Rolla, MO), and the constitutively active form of RhoA, RhoA-V14, inserted into pEGFP-C1, was generously provided by Prof. E. Klussmann (Leibniz-Institut fur Molekulare Pharmakologie, Berlin, Germany). The full-length human ezrin (GenBank accession BC013903) was cloned into pEGFP-N1 via XhoI and EcoRI sites by using the following primers: (forward) CGCCTCGAGATGCCGAAACCAATCAATGTC/CTGAATTCGCAGGGCCTCGAACTCGTC (reverse). The mutation of threonine 567 to alanine (T567A) was produced by site-direct mutagenesis by using the primer CGGGACAAGTACAAGgccCTGCGGCAGATCCG. All of these clones behave as dominant mutants over the endogenous protein.

Levels of construct expression were analyzed by immunostaining for 6-His-tag (NHERF1 constructs), for green fluorescent protein (GFP) (ezrin and RhoA-V14 constructs), or for HA (RhoA-N19 construct), and the transfection level was ~60%. Furthermore, treatment with Escort IV reagent or transfection with the empty vector (pcDNA3.1 or pEGFP-C1) did not significantly change either F-actin levels or the CFTR-dependent chloride efflux measurements with respect to that measured in nontransfected cells (control) [16HBE14o- F-actin content measurements: control: 4.02 ± 0.09, n = 7; Escort IV: 3.98 ± 0.009, n = 5; pcDNA3.1: 3.92 ± 0.12, n = 4; and pEGFP: 3.89 ± 0.17, n = 7, fluorescence intensity/μg protein; and CFTR-dependent chloride efflux: control: 0.0238 ± 0.0026, n = 5; Escort IV: 0.0213 ± 0.003, n = 7; pcDNA3.1: 0.022 ± 0.002, n = 3; and pEGFP: 0.023 ± 0.003, n = 4, $\Delta(F/F_0)$/min]. Transfection with small interfering RNA (siRNA) targeting NHERF1 (siGENOME Smart pool reagent; Dharmacon RNA Technologies, Lafayette, CO) or with scrambled siRNA (Dharmacon RNA Technologies) as a control was performed using Lipofectamine 2000 reagent according to the manufacturer's protocol, and the experiments were conducted 72 h later.

Development of a Stable Transfected Cell Line Overexpressing wt NHERF1

wt NHERF1 and pcDNA3.1 empty vector cDNAs were transfected into CFBE41o- cells by using Escort IV reagent according to the manufacturer's

protocol. After 48 h, cells were diluted by 1:20, 1:40, and 1:80 into 100-mm dishes containing growth complete medium supplemented with 400 μg of hygromycin B, which corresponded to the lowest concentration of drug that began to give massive cell death in 3 d and killed all the cells within 2 wk. The selective medium was replaced every 4 d. After 2–4 wk, isolated colonies appeared, and the largest colonies were picked and placed into wells of a 48-well plate containing selective medium. Clones isolated after hygromycin B selection were screened by Western blotting, F-actin content, and fluorescence measurements of apical chloride efflux. One of the 11 clones overexpressing wt NHERF1, the selected clone (CFBE41o-/sNHERF1), exhibited 1) the highest NHERF1 expression level, 2) a higher expression level of mature band of F508del CFTR with respect to the immature band, and 3) a significant rescue of CFTR-dependent chloride secretion (Supplemental Figures 1S and 2S).

Fluorescence Measurements of Apical Chloride Efflux

Chloride efflux was measured using the Cl^--sensitive dye MQAE. Confluent cell monolayers were loaded overnight in culture medium containing 5 mM MQAE at 37°C in a CO_2 incubator and then inserted into a perfusion chamber that allowed independent perfusion of apical and basolateral cell surfaces. The apical Cl^- efflux measurements were performed when the confluent cell monolayers reached a transepithelial resistance $>300\ \Omega \times cm^2$ measured with the Millicell-ERS; Electrical Resistance System, Millipore). Fluorescence was recorded with a Cary Eclipse spectrofluorometer (Varian, Palo Alto, CA). To measure chloride efflux rate across the apical membrane, the apical perfusion medium was changed with a medium in which chloride was substituted with iso-osmotic nitrate. All experiments were performed at 37°C in HEPES-buffered bicarbonate-free media [Cl^- medium: 135 mM NaCl, 3 mM KCl, 1.8 mM $CaCl_2$, 0.8 mM $MgSO_4$, 20 mM HEPES, 1 mM KH_2PO_4, 11 mM glucose, and Cl^- free-medium: 135 mM $NaNO_3$, 3 mM KNO_3, 0.8 mM $MgSO_4$, 1 mM KH_2PO_4, 20 mM HEPES, 5 mM $Ca(NO_3)_2$, and 11 mM glucose). We measured the apical CFTR-dependent chloride secretion as described previously (Guerra et al., 2005): CFTR-dependent chloride secretion was calculated as the difference in the rate of change of FSK- plus IBMX-stimulated fluorescence in the absence or presence of apical treatment with the specific CFTR inhibitor $CFTR_{inh}$-172 (Ma et al., 2002; Taddei et al., 2004) (Supplemental Figure 3S).

F-Actin Content in Adherent Cells

Actin polymerization assay was performed as described previously (Korichneva and Hammerling, 1999; Paradiso et al., 2004). In brief, confluent cells, grown on coated 35-mm dishes, were fixed with 3.7% formaldehyde and permeabilized in 0.1% Triton X-100 in phosphate-buffered saline (PBS). The cells were then incubated with 0.25 μM phalloidin-TRITC in buffer containing 20 mM KH_2PO_4, 2 mM $MgCl_2$, 5 mM EGTA, and 10 mM PIPES (pH 6.8 with KOH) for 1 h. Cells were incubated in methanol at 4°C overnight to extract phalloidin linked to F-actin. After extraction, plated cells were washed with PBS, and a Bradford Coomassie Plus Protein Assay (Pierce Chemical) was performed to determine total cell protein in the sample. Fluorescence of the methanol extraction solution for each sample was recorded at 540 nm excitation and 565 nm emission with a Cary Eclipse plate reader (Varian). The emission measurements were normalized to protein levels for each sample.

Coimmunoprecipitation and Western Blotting

Confluent monolayers of indicated cell types or treatments, grown on coated 60-mm dishes, were lysed in coimmunoprecipitation buffer (50 mM Tris, 100 mM NaCl, 1 mM EDTA, 5 mM $MgCl_2$, 10% (vol/vol) glycerol, 0.5% (wt/vol) sodium deoxycholate, and 1% Triton X-100 (pH 7.4 with HCl) plus a protease inhibitor mixture (Sigma-Aldrich). The cell lysates were clarified by centrifugation at 10,000 $\times$ *g* for 5 min at 4°C. An aliquot of 300 μg of protein was incubated with the anti-ezrin monoclonal antibody (mAb) (2 μg) or with the anti-NHERF1 polyclonal antibody (2 μg) in rotation overnight at 4°C followed by addition of 50 μl of Dynabeads-protein A conjugates (Dynal, Invitrogen) for an additional 2 h. Immunocomplexes were washed with PBS and then eluted in Laemmli buffer, heated at 95°C for 5 min. Samples were then fractionated by SDS-polyacrylamide gel electrophoresis (PAGE) (NuPAGE Novex 4–12% Bis-Tris Midi Gel; Invitrogen) and electroblotted to polyvinylidene difluoride membranes (GE Healthcare, Little Chalfont, Buckinghamshire, United Kingdom). Proteins were probed by appropriate primary (CFTR, 1:500; ezrin, 1:250; or β-actin, 1:5000) and secondary antibodies and detected using enhanced chemiluminescence (GE Healthcare). Densitometric quantification and image processing were carried out using Photoshop (Adobe Systems, Mountain View, CA) and the NIH Image software package version 1.61 (National Institutes of Health, Bethesda, MD).

Cell Fractionation

Fractionation was performed essentially as described previously (Korichneva *et al.*, 1995), with the addition that cytosolic proteins were prepared by concentrating the supernatants through Centricon Centrifugal Filter Devices YM-10, 10,000 molecular weight cut-off (Millipore). An aliquot of 7 μg of protein from each membrane, cytosolic, and cytoskeletal fraction was diluted in Laemmli buffer, heated at 95°C for 5 min, and separated by 9% Tris-HCl SDS-PAGE. The primary antibodies used were anti-human ezrin (dilution 1:250) and polyclonal anti-human phospho-Ezrin (Thr567)/Radixin (Thr564)/Moesin (Thr558) (dilution 1:1000). Marker proteins for each fraction were used to analyze the amount of cross-contamination from one fraction to another. The blots were probed with anti-Na^+/K^+-ATPase α-1, clone C4646 (dilution 1:10000), anti-HSP70 (dilution 1:250), and anti-α-actinin (dilution 1:1000). No contaminating immunoreactive bands were detected in any of the blots (Supplemental Figure 4S).

Immunofluorescence and Confocal Analysis

Polarized cell monolayers were fixed in 3.7% paraformaldehyde and permeabilized in 0.1% Triton X-100 in PBS. The permeabilization was omitted for monolayers of cells stained for anti-CFTR (CF3) mouse monoclonal (dilution 1:500). To analyze the distribution of phosphorylated ERM, monolayers were incubated with polyclonal anti-human phospho-Ezrin (Thr567)/Radixin (Thr564)/Moesin (Thr558) (dilution 1:100) according to the manufacturer's protocol. Goat anti-rabbit immunoglobulin (IgG) conjugated to Alexa Fluor 488 (dilution 1:1000) was used as secondary antibody for phospho-ezrin, and goat anti-mouse IgG conjugated to Alexa Fluor 568 (dilution 1:1000) was used for CFTR. Monolayers were stained with 20 nM phalloidin-TRITC to visualize F-actin. Monolayers were then mounted onto slides with VECTASHIELD mounting medium (Vector Laboratories, Burlingame, CA) and examined with an Axioskop microscope (Carl Zeiss, Jena, Germany) equipped with a laser scanning confocal unit model MRC-1024 containing a 15-mW krypton-argon laser (Bio-Rad Laboratories, Hercules, CA). Specimens were viewed through a Planapo 63×/1.4 oil immersion objective, and images were acquired in the horizontal (xy) and in the vertical (xz) planes by the Laser Sharp 2000 program (Bio-Rad Laboratories). xy sections were taken at ~2 μm from the top, whereas xz sections were acquired at random.

In Vitro Assay for RhoA Activity

RhoA activity was assessed as described previously (Cardone et al., 2005) by using the RhoA-binding domain of Rhotekin in a kit supplied from Millipore. In brief, 16HBE14o-, CFBE41o- transfected or not with cDNA for NHERF1-ΔERM and CFBE41o- stably overexpressing NHERF1 cells, plated on coated 60-mm dishes, were washed with PBS and extracted with radioimmunoprecipitation assay buffer (50 mM Tris, pH 7.2, 500 mM NaCl, 1% Triton X-100, 0.5% sodium deoxycholate, 1% SDS, 10 mM $MgCl_2$, 0.5 μg/ml leupeptin, 0.7 μg/ml pepstatin, 4 μg/ml aprotinin, and 2 mM phenylmethylsulfonyl fluoride or phenylmethanesulfonyl fluoride). After centrifugation at 14,000 $\times$ *g* for 10 min, supernatant protein concentration was measured by Bradford method (Bradford, 1976), and an aliquot of 600 μg of each protein extract was incubated for 45 min at 4°C with 30 μg of glutathione beads coupled with glutathione transferase–Rho-binding domain (GST-RBD) fusion protein, and then washed with Tris buffer, pH 7.2, containing 1% Triton X-100, 50 mM Tris, 150 mM NaCl, and 10 mM $MgCl_2$. The RhoA content in these samples or in 30 μg of protein of cell homogenate was determined by immunoblotting samples using mouse anti-RhoA antibody (1:500).

In Vivo Fluorescence Resonance Energy Transfer (FRET) Assay for RhoA Activity

FRET microscopy was used to monitor RhoA activity by using the Raichu 1297 probe as described previously (Cardone *et al.*, 2005). In brief, this probe consists of the RBD of the RhoA effector protein Rhotekin, sandwiched between yellow fluorescent protein (YFP) and cyan fluorescent protein (CFP). The intramolecular binding of endogenous GTP-RhoA to the RBD of Rhotekin displaces YFP and CFP, thereby decreasing FRET efficiency between the fluorophores, whereas a reduction of intracellular active RhoA results in the opposite effect. The activity of RhoA is monitored by measuring CFP (480 nm)/YFP (545 nm) fluorescence emission values upon excitation of the transfected cells at 430 nm. To eliminate the distracting data from regions outside of cells, the YFP channel is used as a saturation channel. The ratio images are presented in pseudocolor mode and ratio intensity is displayed stretched between the low and high renormalization value, according to a temperature-based lookup table with red (hot) and blue (cold), indicating, respectively, high and low values of RhoA activity (Figure 9D). Forty-eight hours after transfection, living cells were imaged with an ECLIPSE TE 2000-S microscope (Nikon, Tokyo, Japan) equipped with a cooled charge-coupled device camera controlled by the Metafluor 4.6 software (Meta Imaging 4.6; Molecular Devices, Sunnyvale, CA). The setup of the microscope and the filters used for dual emission imaging studies were described recently (Cardone *et al.*, 2005). After background subtraction, sensitized FRET off-line image analysis of CFP/YFP ratio images was performed with the MetaMorph software (Meta Imaging 4.6; Molecular Devices). Correction of FRET measurements for spectral bleed-through and cross excitation was calculated as ICFP/nF as described previously (Cardone *et al.*, 2005).

Internalization Assay

Endocytosis assay was performed in indicated cell types or treatments grown on 35-mm permeable supports as described previously (Swiatecka-Urban *et al.*, 2002; Silvis *et al.*, 2009). The same cell line was seeded on three filters for every condition. Experiments were performed in a cold room on ice with all

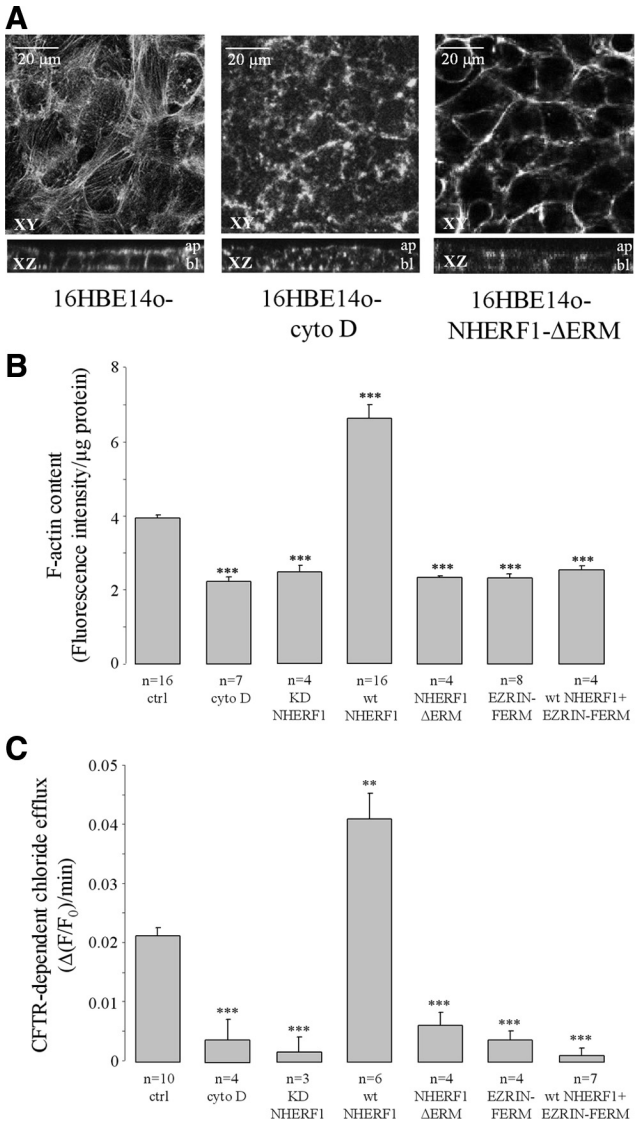

Figure 1. NHERF1-dependent regulation of F-actin organization, assembly and CFTR-dependent chloride secretion in 16HBE14o- cells. (A) Confocal immunofluorescence microscopy was performed in 16HBE14o- polarized cell monolayers grown on permeable filters in control condition (16HBE14o-), treated for 30 min with the F-actin polymerization inhibitor cytochalasin D (cyto D) or transiently transfected with cDNA encoding NHERF1 in which the C-terminal domain that interacts with ezrin is deleted (NHERF1-ΔERM). F-actin was detected by phalloidin-TRITC. Treatment with 20 μM cytochalasin D or transfection with NHERF1-ΔERM altered F actin organization. The horizontal section (xy) was taken at the apical level ~2 μm from the top of the monolayer. The vertical section (xz) was randomly acquired. Ap, location of apical region; bl, location of basal region. (B) F-actin assembly was detected by an actin polymerization assay (see *Materials and Methods*) and expressed as fluorescence intensity normalized to protein content of each sample. Histogram summarizing F-actin content in nontransfected cells (ctrl) or cells transiently transfected with the following constructs: wt NHERF1, cells transfected with cDNA encoding wild-type NHERF1; KD NHERF1, cells transfected with short interfering RNA for NHERF1; NHERF1-ΔERM; Ezrin-FERM, cells transfected with cDNA encoding the FERM-GFP domain of ezrin; and wt NHERF1+Ezrin-FERM, cells cotransfected with cDNAs encoding both NHERF1 and FERM-GFP or cells treated with cyto D. Cells transfected with the empty vectors behaved as the nontransfected cells (see *Materials and Methods*). (C) Summary of CFTR-dependent chloride effluxes measured in 16HBE14o- cell monolayers analyzed in the various experimental conditions reported above. CFTR-dependent chloride transport was calculated from the difference in alterations of FSK-stimulated fluorescence measurements in the absence and presence of the CFTR inhibitor, $CFTR_{inh}$-172 (see *Materials and Methods* and Supplemental Figure 3S). Each bar represents the mean ± SE. Statistical comparison was made using Student's *t* test with respect to the values obtained in nontreated cells: ***p < 0.0001, **p < 0.001.

solutions at 4°C. In brief, cells were rinsed with ice-cold PBS containing 0.1 mM $CaCl_2$ and 1 mM $MgCl_2$ (PBS-CM) and then incubated with 1 mg/ml EZ-LinkSulfo-NHS-SS-Biotin (Pierce Chemical) in borate buffer (85 mM NaCl, 4 mM KCl, and 15 mM $Na_2B_4O_7$, pH 9.0) for 30 min with gentle agitation. Excess biotin was removed with two 10-min washes in PBS-CM containing 10% fetal bovine serum followed by one wash in PBS-CM. To assay the internalization of cell surface CFTR, after biotinylation cells were warmed to 37°C for 1, 2.5, and 5 min. Some filters were kept at 4°C for the cell surface labeling and stripping controls. At the indicated time points, cells were rapidly cooled and biotin molecules exposed at the cell surface after incubation at 37°C were cleaved of biotin with three 10-min washes in impermeant stripping solution (50 mM sodium 2-mercaptoethane-sulfonate [MESNA]), 150 mM NaCl, 1 mM EDTA, 0.2% bovine serum albumin, and 20 mM Tris, pH 8.6) followed by cell lysis. Cells were lysed in biotinylation lysis buffer (BLB: 0.4% deoxycholate, 1% NP-40, 50 mM EGTA, 10 mM Tris-Cl, pH 7.4, and Protease Inhibitor Cocktail; Sigma-Aldrich). Cells scraped from three inserts were unified in one Eppendorf. Lysates were centrifuged (10,000 × *g*) to remove cell debris, and total protein levels were determined. Equivalent amounts of cell lysates (1.5 mg) were incubated overnight with 150 μl of streptavidin (Pierce Chemical). Precipitated proteins were washed three times with BLB, solubilized with Laemmli sample buffer, separated on a 4–12% SDS-PAGE, and blotted for CFTR.

Data Analysis

Data are presented as mean ± SE for the number of samples indicated (n). Statistical comparisons were made using unpaired data Student's *t* test. Differences were considered significant when $p < 0.05$.

RESULTS

We have demonstrated previously that NHERF1 overexpression has an important role in regulating the activity and the apical expression of CFTR in human bronchial 16HBE14o- cell monolayers that express wt CFTR, and, importantly, increases the F508del CFTR expression on the apical membrane and rescues CFTR-dependent chloride efflux in human bronchial (F508del/F508del) CFBE41o- cell monolayers (Guerra *et al*., 2005).

Although CFTR membrane expression and activity have been demonstrated to be dependent on F-actin cytoskeletal organization (Ganeshan *et al*., 2007; Okiyoneda and Lukacs, 2007) and it is known that NHERF1 mediates associations between CFTR and the cytoskeleton via the actin binding protein ezrin (Short *et al*., 1998; Moyer *et al*., 1999; Haggie *et al*., 2004), the role of NHERF1 in regulating the dynamics of cytoskeleton organization still needs to be defined.

Role of NHERF1 Overexpression in Regulating CFTR-dependent Chloride Secretion and the F-Actin Organization and Assembly

16HBE14o- Cells. We first determined the F-actin organization in polarized 16HBE14o- monolayers stained with phalloidin-TRITC that in the XY plane displayed bundled F-actin filaments that seemed to be distributed in the basolateral and apical areas when the entire volume of the cells was analyzed by *z*-axis projection of the confocal images (Figure 1A). Treatment with the F-actin polymerization inhibitor cytochalasin D disorganized the actin filaments (Figure 1A) and reduced F-actin content (Figure 1B) and CFTR-dependent chloride secretion (Figure 1C), confirming that disruption of the cytoskeleton impairs cAMP-dependent activation of CFTR in 16HBE14o- cell monolayers as has been observed in other cell lines (Prat *et al*., 1995; Ganeshan *et al*., 2007).

When we analyzed whether forced alterations in NHERF1 expression in 16HBE14o- cells may influence F-actin assembly and CFTR-dependent chloride efflux, we observed that NHERF1 overexpression not only greatly stimulated CFTR activity (Figure 1C), as we have shown previously (Guerra *et al*., 2005), but also increased the F-actin content (Figure 1B). In contrast, treatment with NHERF1-specific siRNA (KD NHERF1) that significantly reduced the level of endogenous NHERF1 by ~65% and decreased the expression of the fully glycosylated, mature band C of CFTR without affecting wt CFTR overall expression (Supplemental Figure 5S, A and B), significantly reduced F-actin assembly (Figure 1B) and completely inhibited CFTR-dependent chloride secretion (Figure 1C), confirming that NHERF1 plays a positive role in regulating the surface expression of wt CFTR. The nonsilencing, control siRNA had no effect on either F-actin content (4.04 ± 0.18, fluorescence intensity/μg protein, n = 4) or CFTR activity [0.019 ± 0.004 $\Delta(F/F_0)$/min, n = 3].

To explore the possibility that NHERF1 may influence F-actin organization and CFTR-secretion via the mediation of ezrin, we transfected 16HBE14o- cells with cDNA encoding NHERF1 in which the C terminus ezrin interacting domain is deleted (NHERF1-ΔERM), and we found that this experimental condition significantly dissipated most of the cortical actin filaments (Figure 1A, right), reduced F-actin content (Figure 1B), and, as reported previously by us (Guerra *et al*., 2005), decreased apical CFTR-dependent chloride secretion (Figure 1C), whereas transfection with empty vector had no effect on any of these parameters (see *Materials and Methods*).

In analogy to that observed with NHERF1-ΔERM, transfection of 16HBE14o- cells with the FERM domain of ezrin bound to GFP (Ezrin-FERM), which blocks ezrin interaction with actin and functions as a dominant negative of ezrin (Stanasila *et al*., 2006), significantly reduced both F-actin content and CFTR-dependent chloride secretion (Figure 1, B and C). Importantly, cotransfection of wt NHERF1 together with Ezrin-FERM reversed the increase of F-actin content and CFTR-dependent chloride efflux induced by wt NHERF1 overexpression, demonstrating that NHERF1 overexpression increases both cytoskeleton organization and CFTR–dependent chloride secretion only when it can interact with actin through the mediation of ezrin.

CFBE41o- Cells. The above-mentioned results, together with the previous findings demonstrating that NHERF1 was less expressed in CFBE41o- cells compared with 16HBE14o- cells (Guerra *et al*., 2005), suggest the possibility that NHERF1 overexpression in CFBE41o- cells could rescue functional apical chloride secretion through the ezrin-mediated regulation of the actin cytoskeleton. To verify this, we analyzed the cytoskeleton organization in CFBE41o- cells stably overexpressing wt NHERF1 (CFBE41o-/sNHERF1) and in CFBE41o- cells stably transfected with empty pcDNA3.1 vector, called control CFBE41o- (see *Materials and Methods* and Supplemental Figure 1S and 2S).

As shown in Figure 2A, control CFBE41o- cell monolayers displayed substantial disorganization of actin filaments in punctate fluorescent structures, whereas in CFBE41o-/sNHERF1 cells, NHERF1 overexpression induced a small increase in cortical actin filaments and a significant increase in the F-actin content (Figure 2B) and apical CFTR-dependent chloride efflux (Figure 2C) with respect to CFBE41o- control cells. Cytochalasin D treatment of CFBE41o-/sNHERF1 cells, in analogy to that seen in 16HBE14o- cells, reduced both F-actin levels and CFTR-dependent chloride

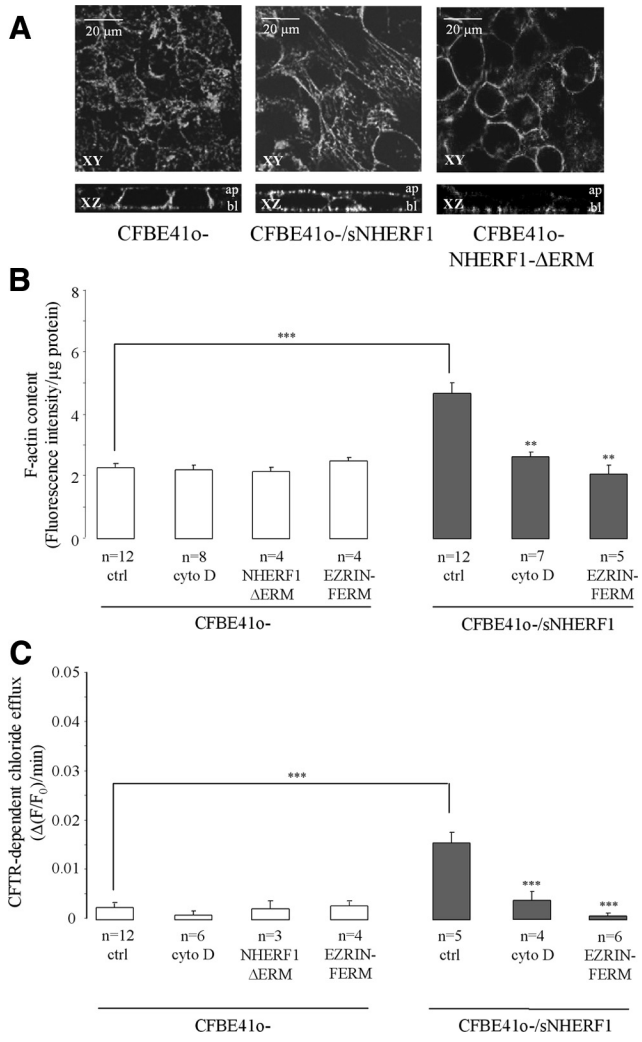

Figure 2. NHERF1 overexpression-dependent increase of F-actin organization, assembly and CFTR dependent chloride secretion in CFBE41o- cells. (A) Confocal immunofluorescence microscopy of control CFBE41o- monolayers displayed substantial disassembly of actin filaments into punctate fluorescent structures. Stable overexpression of wt NHERF1 in CFBE41o- cells (CFBE41o-/sNHERF1) partially restored the F-actin organization, as demonstrated by an increased actin staining at the apical pole of the cells in projections of the *z*-axis stack of the confocal images, whereas transfection of CFBE41o- cell monolayers with NHERF1-ΔERM had no effect on the F-actin organization. The horizontal section (xy) at the apical level was taken at 2 μm from the top of the epithelial monolayer. The vertical section (xz) was randomly acquired. ap, location of apical region; bl, location of basal region. F-actin levels (B) and CFTR-dependent chloride efflux measurements (C) were performed in CFBE41o- and in CFBE41o-/sNHERF1 cells in the indicated experimental conditions. Each bar represents the mean ± SE. Statistical comparisons were made using Student's *t* test: ***$p < 0.0001$, **$p < 0.001$ versus nontreated CFBE41o-/sNHERF1.

secretion but had no effect in control CFBE41o- cells (Figure 2, B and C).

To explore the possibility that ezrin mediates this NHERF1 overexpression-dependent increase of F-actin assembly and CFTR-dependent chloride secretion in CFBE41o-/sNHERF1 cells, control CFBE41o- were transfected with cDNA encoding NHERF1-ΔERM. As can be seen in Figure 2, NHERF1-ΔERM failed to increase F-actin organization (Figure 2A) and did not change the low values of either F-actin content or CFTR-de-

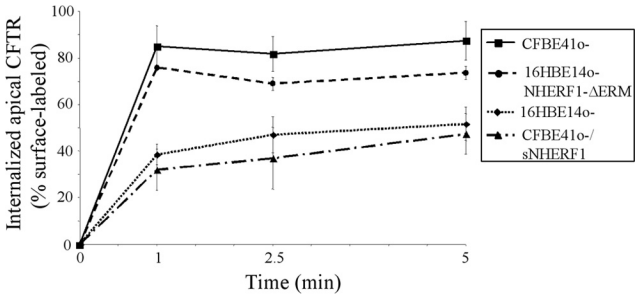

Figure 3. Effect of NHERF1 overexpression and its interaction with ezrin on the kinetics of CFTR internalization. Polarized cell monolayers grown on permeable filters were biotinylated at 0°C and warmed to 37°C for the indicated times and the labeled CFTR remaining at the cell surface was stripped by MESNA. Internalized CFTR signals were normalized to the respective surface CFTR signals and plotted as a function of time. The data points represent mean ± SE of three experiments.

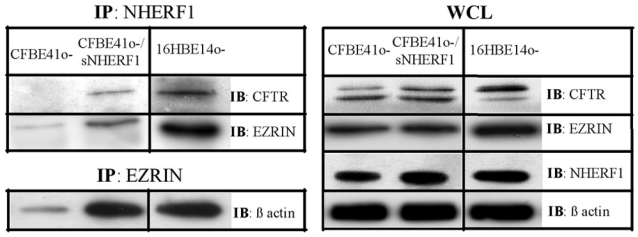

Figure 4. NHERF1 overexpression modulates CFTR-NHERF1, NHERF1–ezrin, and ezrin–actin interactions. The interaction between NHERF1 and CFTR, NHERF1, and ezrin as well as between ezrin and actin were measured in coimmunoprecipitation experiments as described in *Materials and Methods*. Representative blots show immunoprecipitates (IP) obtained with polyclonal NHERF1 antibody and immunoblotted (IB) with monoclonal CFTR antibody (n = 3) or monoclonal ezrin antibody (n = 4) or immunoprecipitates with monoclonal ezrin antibody and immunoblotted with monoclonal β-actin antibody (n = 4) in CFBE41o-, CFBE41o-/sNHERF1 cells. In 16HBE14o- cells immunoprecipitation was performed for three times. Right, respective whole cell lysates (WCL).

pendent chloride efflux found in control CFBE41o- cells (Figure 2, B and C). Similarly, transfection of control CFBE41o- cells with the cDNA encoding Ezrin-FERM also did not change either the F-actin content or the PKA-dependent CFTR secretion.

Importantly, in analogy to that observed in 16HBE14o- cells, the NHERF1 overexpression-induced increase in both F-actin content and CFTR-dependent chloride efflux observed in CFBE41o-/sNHERF1 cells was completely reversed by transfection with the Ezrin-FERM domain, demonstrating that the NHERF1 overexpression-induced increase of these two processes in CFBE41o- cells also depends on the capability of NHERF1 to interact with the actin cytoskeleton via the mediation of ezrin.

NHERF1 Overexpression Affects the Kinetics of CFTR Internalization

We have observed previously that NHERF1 overexpression in 16HBE14o- and CFBE41o- cell monolayers increases the surface apical expression of both wt and F508del CFTR as measured by apical biotinylation and concluded that this increase could explain the NHERF1-induced increase of CFTR activity measured in both 16HBE14o- and CFBE41o- cell monolayers (Guerra *et al*., 2005). Therefore, we next determined whether that increase of surface expression could be explained by a NHERF1-dependent regulation of wt and F508del CFTR endocytosis. To this end, we analyzed the rate of endocytosis in polarized cell monolayers of 16HBE14o- or 16HBE14o- expressing NHERF1-ΔERM monolayers, as well as in control CFBE41o- and in CFBE41o-/sNHERF1 monolayers by using the biotin protection assay described in *Materials and Methods* (Figure 3). In the control CFBE41o- cells, which have a low but measurable cell surface expression of F508del CFTR protein in the apical membrane (Guerra *et al*., 2005), a larger fraction of surface-labeled F508del CFTR was internalized in the first 2.5 min. The overexpression of wt NHERF1 (CFBE41o-/sNHERF1, triangles) decreased F508del CFTR internalization to levels similar to that found for wt CFTR in 16HBE14o- cells (diamonds). Moreover, transfection of 16HBE14o- cells with NHERF1-ΔERM (circles) greatly increased wt CFTR internalization to levels similar to those observed in control CFBE41o- (squares) cell monolayers, suggesting that NHERF1 greatly influences both wt CFTR and F508del CFTR internalization through its interaction with the actin cytoskeleton via ezrin.

NHERF1 Overexpression Increases NHERF1-Ezrin-Actin Interactions in CFBE41o- Cells

To investigate whether NHERF1 overexpression in CFBE41o- cells may directly regulate the association between the various components of the signal complex CFTR-NHERF1-ezrin-actin, we performed a series of coimmunoprecipitation experiments in control CFBE41o- and CFBE41o-/sNHERF1 cells (Figure 4). Coimmunoprecipitation with anti-human NHERF1 followed by Western blotting analysis of the resulting immunoprecipitates with anti-human CFTR or anti-human ezrin showed that the interaction between NHERF1 and CFTR as well as between NHERF1 and ezrin was significantly higher in CFBE41o-/sNHERF1 than in control CFBE41o- cells (2.85 ± 0.11-fold increase, n = 3, $p < 0.01$ and 3.13 ± 0.15-fold increase, n = 4, $p < 0.001$, respectively, for the NHERF1-CFTR and the NHERF1-ezrin interactions). Furthermore, coimmunoprecipitation of cell homogenates with anti-ezrin followed by Western blotting with anti-β-actin (Figure 4, bottom left) showed that NHERF1 overexpression significantly increased the interaction of ezrin with actin (3.03 ± 0.13-fold increase, n = 4, $p < 0.001$). Interestingly, as seen in Figure 4, the pattern of interaction between CFTR-NHERF1-ezrin-actin found in CFBE41o-/sNHERF1 cells was similar to that found in 16HBE14o- cells.

Furthermore, analysis of whole cell lysates (Figure 4, WCL, right) demonstrated that stable transfection of control CFBE41o- cells with wt NHERF1 increased NHERF1 expression (178.10 ± 11.30%, n = 7, $p < 0.001$), whereas not significantly changing total ezrin, actin, or overall CFTR expression (115.52 ± 8.09%, n = 3; 104.93 ± 6.41%, n = 4; and 92.71 ± 4.72%, n = 4 for CFTR, ezrin, and actin, respectively).

As seen in the top panels of Figure 5A, the increase of the interaction between NHERF1 and actin observed in CFBE41o-/sNHERF1 cells, was compromised when control CFBE41o- cells were transfected with cDNA encoding NHERF1-ΔERM. The phosphorylation of the C-terminal Thr567 residue in ezrin is important in maintaining it in an "open" form where its C terminus can bind F-actin and its N terminus can bind NHERF1 (Bretscher *et al*., 1997; Matsui *et al*., 1998). As seen in the bottom panels of Figure 5B, blocking ezrin phosphorylation via transfection of CFBE41o-/sNHERF1 cells with cDNA encoding for the phospho-dead ezrin mutant, T567A, which cannot be phosphorylated, resulted in a significantly lower interaction between NHERF1 and actin in CFBE41o-/sNHERF1, demonstrating that the phosphorylation

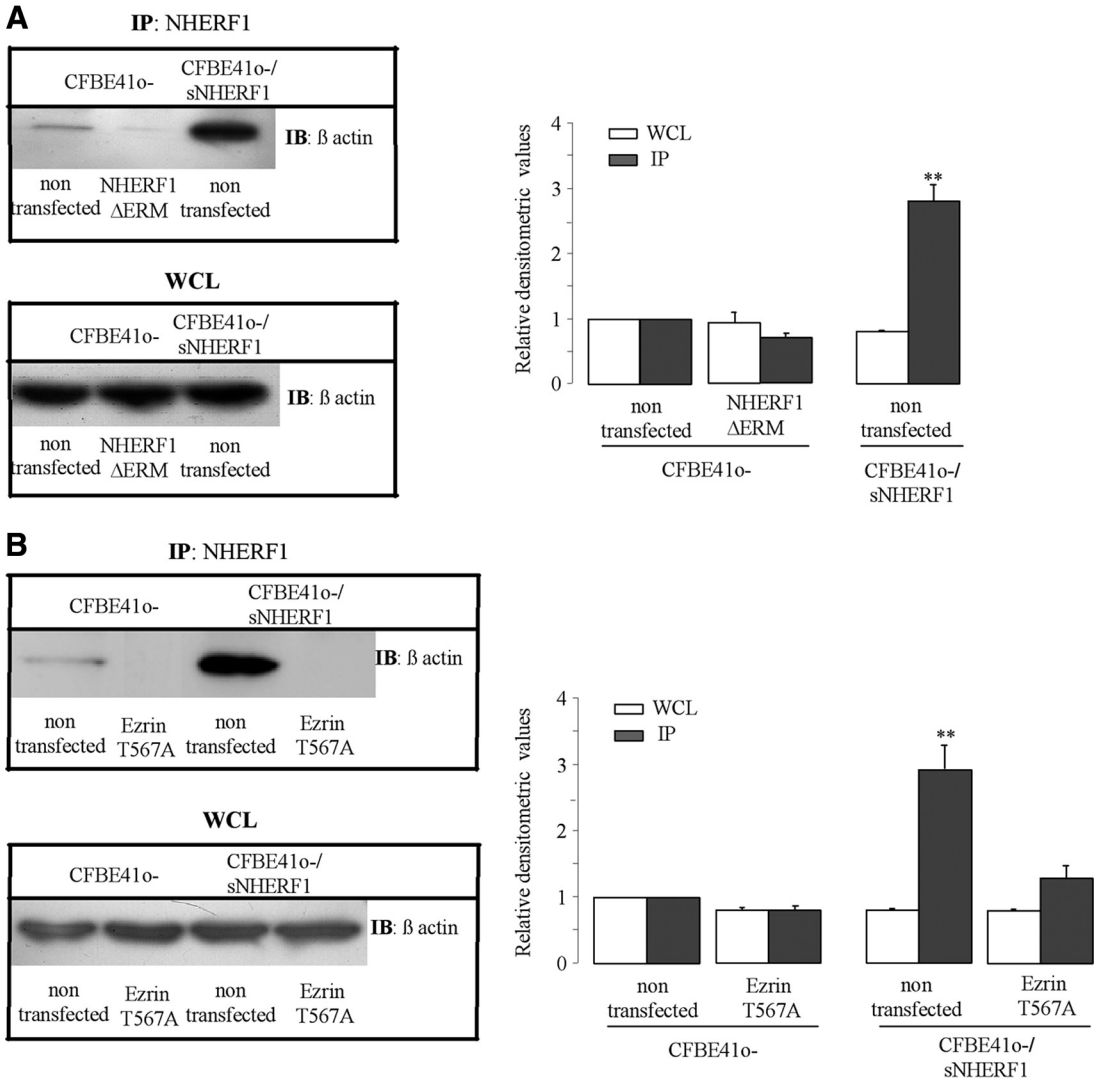

Figure 5. NHERF1-actin interaction was compromised in cells transfected with NHERF1-ΔERM or with nonphosphorylable ezrin cDNAs. A representative blot (left) and histogram summarizing relative densitometric values (right) are shown for immunoprecipitates with polyclonal NHERF1 antibody and immunoblotted with monoclonal β-actin antibody in CFBE41o-, CFBE41o-/sNHERF1, and CFBE41o- cells transfected with the cDNA encoding NHERF1-ΔERM (n = 3) (A); and immunoprecipitates with NHERF1 antibody and immunoblotted with actin antibody in CFBE41o- and CFBE41o-/sNHERF1 cells transfected or not with cDNA encoding for the nonphosphorylable ezrin mutant T567A (n = 4) (B), **$p < 0.001$ versus nontransfected CFBE41o- cells.

of ezrin at Thr567 is a key step in the formation of the multiprotein complex NHERF1-ezrin-actin.

NHERF1 Overexpression Relocalizes Phospho-ERM Proteins in CFBE41o- Cells

Therefore, we next examined phospho-ezrin distribution in both control CFBE41o- and CFBE41o-/sNHERF1 cell monolayers with a phospho-ERM [ezrin (Thr567)/Radixin (Thr564)/Moesin (Thr558)] antibody. Results obtained in cell fractionation experiments measuring the expression of phosphorylated ezrin (top band, arrowhead corresponding to the phosphorylated ezrin) and total ezrin in the membrane, cytosolic, and cytoskeletal fractions by Western blotting (Figure 6A, top) showed that the overexpression of wt NHERF1 (CFBE41o-/sNHERF1 cells) increased the ratio of phosphorylated to total ezrin in the membrane fraction, and this did not occur in either control CFBE41o- cells or those transfected with NHERF1-ΔERM. These results are in line with the findings that phosphorylated, activated ERM proteins are preferentially targeted to the actin rich membrane structures (Matsui *et al*., 1998; Hayashi *et al*., 1999). Confocal analysis of polarized monolayers on permeable filters (Figure 6A, bottom), confirmed that phospho-ERM proteins were lowly and randomly expressed in control CFBE41o- cells, whereas stable overexpression of wt NHERF1 (CFBE41o-/sNHERF1 cells) led to a significant increase of phospho-ERM expression mainly at the apical region. Interestingly, this apical redistribution of phospho-ERM was dependent on the capability of NHERF1 to interact with the N terminus of ezrin because CFBE41o- cells transfected with the cDNA encoding the NHERF1-ΔERM construct displayed a phospho-ERM distribution similar to that observed in control CFBE41o- cells. Altogether, these results suggest that the overexpression of NHERF1 regulates the intramolecular association of ezrin and its subsequent activation and recruitment in the apical region. Importantly, the hypothesis that NHERF1 overexpression in CFBE41o- cells restores a "normal" phenotype is

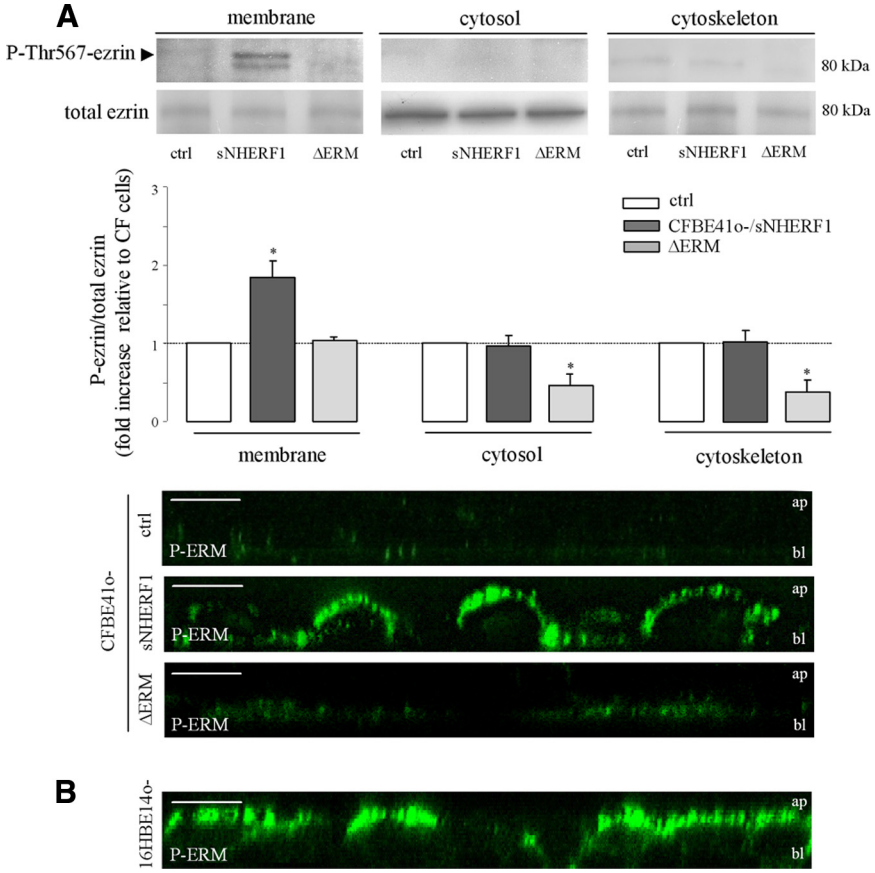

Figure 6. NHERF1 overexpression relocalizes phospho-ERM proteins in CFBE41o- cells. (A) Phospho-ezrin distribution was analyzed with a polyclonal phospho-ERM [ezrin (Thr567)/Radixin (Thr564)/Moesin (Thr558)] antibody: 1) A representative Western blot analysis for P-ezrin at Thr567 (top band, arrowhead corresponding to the phosphorylated ezrin) and total ezrin in membrane, cytosolic, and cytoskeletal fractions of control CFBE41o- cells (ctrl), CFBE41o-/sNHERF1 (sNHERF1), and CFBE41o- transfected with NHERF1-ΔERM cDNA (ΔERM); and 2) graphic representation of phospho-ezrin subcellular distribution, expressed as the phospho-ezrin/total ezrin ratio normalized in each fraction to the level in nontransfected CFBE41o- cells, designated as 1. Data represent means ± SE, n = 7; *p < 0.01, versus nontransfected CFBE41o- cells. 3) Confocal immunofluorescence microscopy was performed on polarized monolayers of CFBE41o-, CFBE41o-/sNHERF1, and CFBE41o- transfected with NHERF1-ΔERM cDNA grown on permeable filters. Phospho-ERM was detected by polyclonal antibody and the images are in the vertical (xz) plane. ap, location of apical region; bl, location of basal region. Bars, 10 μm. (B) Phospho-ERM localization in 16HBE14o- cell monolayers. Confocal immunofluorescence microscopy was performed in polarized 16HBE14o- cells grown on permeable filters. Bars, 10 μm.

supported by the finding that confocal analysis of phospho-ERM distribution in 16HBE14o- cells (Figure 6B) was similar to that found in the CFBE41o-/sNHERF1 cells.

Involvement of RhoA/ROCK Pathway in the Regulation of F-Actin Content and CFTR Activity

RhoA is an important regulator of actin-based cytoskeletal organization (Tapon and Hall, 1997) and, in most cell types, is an upstream activator of ezrin (Matsui *et al*., 1998). In cell fractionation experiments, we observed that transfection with the dominant active mutant of RhoA, RhoA-V14, increased the ratio of phosphorylated to total ezrin in the membrane fraction of CFBE41o- cells similarly to that observed during NHERF1 overexpression (Figure 7). We then analyzed the role of RhoA in regulating F-actin content and CFTR-dependent chloride efflux. Transfection of control CFBE41o- cells with the dominant active RhoA-V14 induced a significant increase of cortical actin filaments (Supplemental Figure 6S) and strongly increased both F-actin content (Figure 8A, white bars) and CFTR-dependent chloride efflux (Figure 8B, white bars), whereas transfection with the dominant negative mutant of RhoA (RhoA-N19) had no effect. To assess if RhoA-V14-dependent rescue of CFTR activity resulted from a redistribution of F508del CFTR from the cytoplasm to the apical membrane, we performed confocal immunofluorescence measurements in nonpermeabilized CFBE41o- polarized cell monolayers stained with an mAb that recognizes a sequence in the first extracellular loop of the human CFTR protein (Bossard *et al*., 2007). As can be seen in Figure 8C, F508del CFTR was highly expressed on the apical membrane of CFBE41o- cell monolayers that had been transfected with RhoA-V14 bound to GFP, whereas nontransfected CFBE41o- monolayers did not show any signal for CFTR membrane expression. Altogether, these data

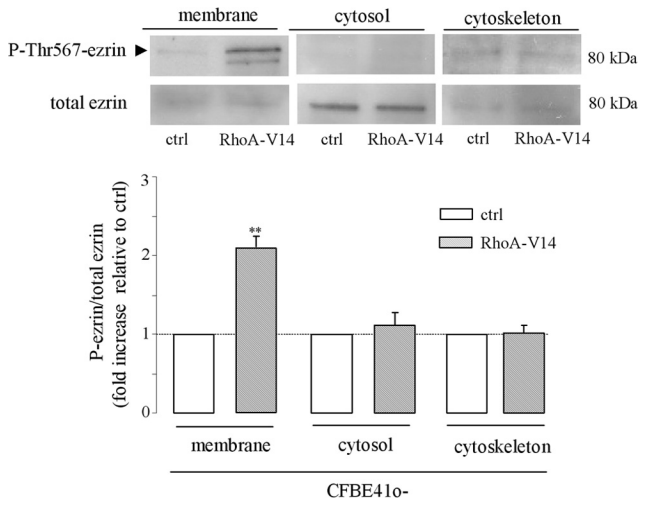

Figure 7. Regulation of phospho-ezrin distribution by RhoA in CFBE41o- cells. A representative Western blot analysis for P-ezrin at Thr567 and total ezrin in membrane, cytosolic, and cytoskeletal fractions of control CFBE41o- cells transfected with the constitutively active mutant of RhoA, RhoA-V14, and histogram representation of phospho-ezrin subcellular distribution in CFBE41o- and CFBE41o- cells transfected with RhoA-V14, expressed as the ratio of phospho-ezrin/total ezrin normalized in each fraction to that in nontransfected CFBE41o- cells, designated as 1. Data are means ± SE, n = 5; **p < 0.001 versus nontransfected cells.

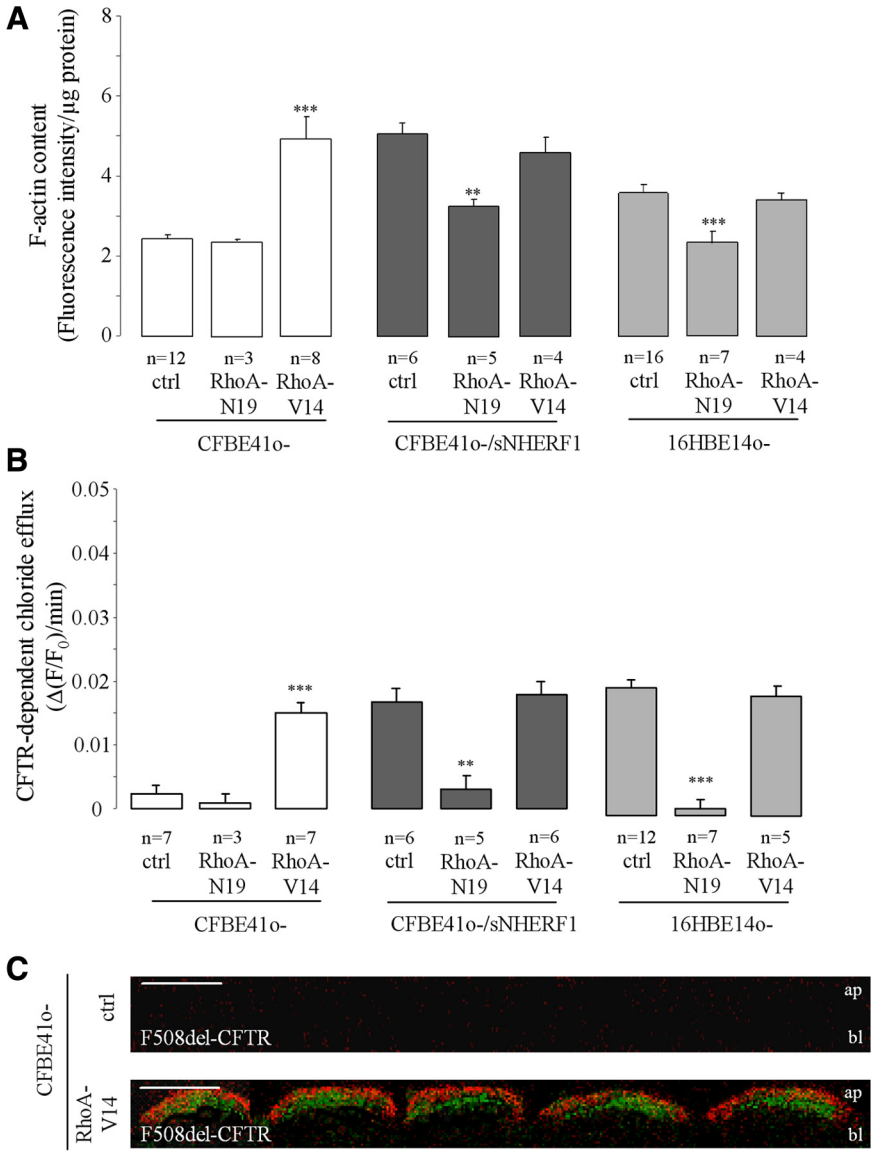

Figure 8. Regulation of F-actin content and CFTR activity mediated by RhoA. (A) Summary of F-actin content measurements performed in CFBE41o- and CFBE41o-/sNHERF1 and 16HBE14o- cells. Each bar represents the mean ± SE; **$p < 0.001$ and ***$p < 0.0001$ versus nontransfected cells. Ctrl, nontransfected cells; RhoA-N19, cells transfected with cDNA encoding dominant-negative RhoA; and RhoA-V14, cells transfected with cDNA encoding constitutively active RhoA. (B) Summary of CFTR-dependent chloride secretion measurements in CFBE41o- cells; CFBE41o-/sNHERF1 cells and 16HBE14o- cells transfected or not with RhoA mutants. CFTR-dependent chloride efflux was calculated as described previously; **$p < 0.001$ and ***$p < 0.0001$ versus nontransfected monolayers. (C) Confocal immunofluorescence microscopy images of polarized CFBE41o- monolayers grown on permeable filters, transfected or not with cDNA for GFP-RhoA-V14 (green). Unpermeabilized cells were immunolabeled with a primary mouse mAb (CF3) raised against the extracellular first loop of CFTR (red), as described in *Materials and Methods*. Confocal scans are shown in the vertical cross-section (xz) plane. ap, location of apical region; bl, location of basal region. Bars, 10 μm.

suggest that in CFBE41o- cells, RhoA activity is very low and its activation is able to rescue both F-actin polymerization and F508del CFTR functional expression in the apical membrane.

Importantly, in identical experiments conducted in both CFBE41o-/sNHERF1 (Figure 8, A and B, black bars) and 16HBE14o- cells (Figure 8, A and B, gray bars), inhibition of RhoA with the dominant-negative mutant RhoA-N19 significantly decreased both F-actin content and CFTR-dependent chloride secretion, whereas RhoA-V14 was ineffective, confirming again that CFBE41o-/sNHERF1 cells behave as 16HBE14o- cells.

The finding that RhoA-V14 in CFBE41o-/sNHERF1 did not cause a further increase in either F-actin content or CFTR activity suggests that NHERF1 is required for RhoA activation. Figure 9A shows a representative blot of a pull-down assay for active RhoA (RhoA-GTP), indicating that RhoA activity is higher in both CFBE41o-/sNHERF1 and 16HBE14o- cells than in control CFBE41o- or CFBE41o- cells transfected with NHERF1-ΔERM. Total RhoA levels in the samples before precipitation were unchanged in the cell lines and were used to normalize changes in RhoA activity for analysis of multiple experiments by using a scanning densitometer (Figure 9B).

These data suggest that NHERF1 can regulate RhoA activation only when it can interact with the N terminus of ezrin through its ERM binding domain. To confirm this hypothesis, we performed FRET microscopy to directly analyze the amount of active RhoA in intact living cells. We measured RhoA activity state by using a single-chain CFP/YFP FRET biosensor for RhoA (pRaichu 1297x) (Yoshizaki *et al*., 2004), which directly monitors the level of the endogenous RhoA-GTP by measuring FRET between the two GFP mutants fused to the RBD of Rhotekin. Using this FRET-based probe, we verified that RhoA activity was significantly higher in CFBE41o-/sNHERF1 cells than in control CFBE41o- or CFBE41o- cells overexpressing NHERF1-ΔERM (Figure 9C).

In most cell types, RhoA acts as an upstream signal molecule to activate ROCK, which, in turn, is involved in phosphorylating ezrin, which maintains ezrin in its active state by preventing its self-association (Matsui *et al*., 1998). In line with the RhoA functional data, a 12-h preincubation of CFBE41o-/sNHERF1 cells with the ROCK selective inhibitor Y-27632 (1 μM) (Uehata *et al*., 1997) significantly inhibited 1)

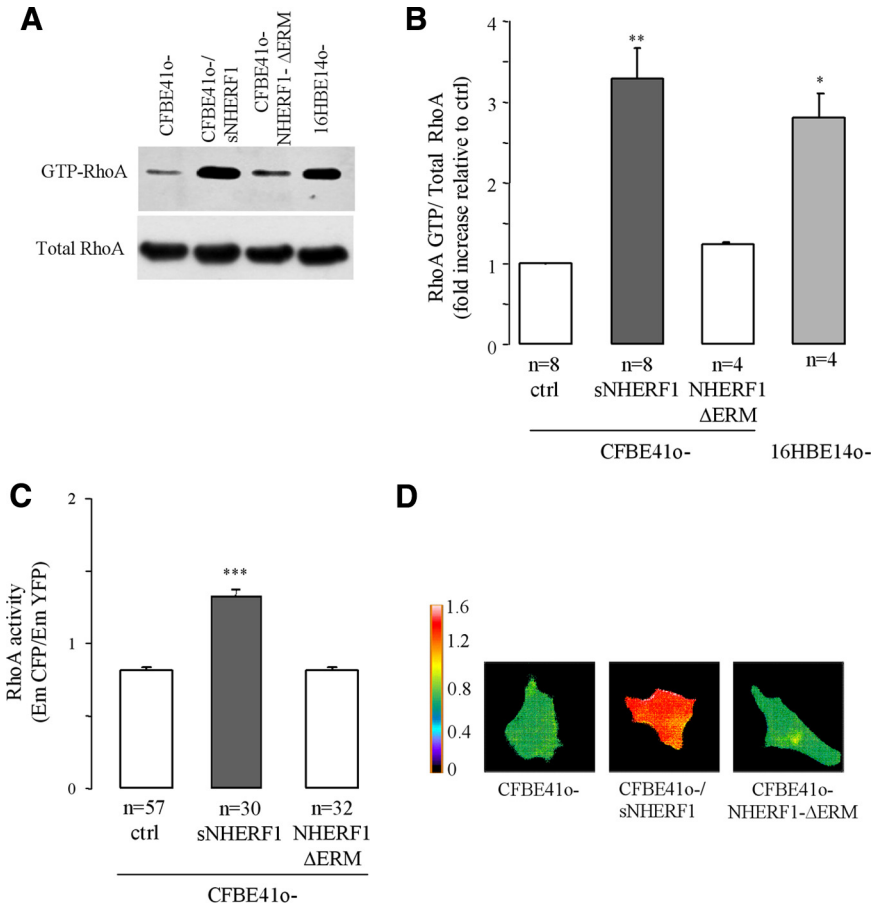

Figure 9. NHERF1 overexpression increases RhoA activity in CFBE41o- cells. RhoA activity was analyzed by pull-down assay by using GST-RBD of Rhotekin (A and B) in CFBE41o- and CFBE41o-/sNHERF1, CFBE41o- transiently transfected with cDNA encoding NHERF1-ΔERM and 16HBE14o- cells. Proteins bound to GST-RBD and total lysates were subjected to SDS-PAGE and immunoblotting by using anti-RhoA antibody. (A) Representative Western Blot of GST-RBD pull-down showing RhoA activity. Bottom, amount of total RhoA in whole cell lysates. (B) Summary of pull-down experiments. The intensity of each band was quantified by image analysis with the NIH Image software package. RhoA activity is expressed as the ratio of GTP-RhoA/total RhoA and normalized to that found in nontransfected CFBE41o- cells designated as 1. Data are means ± SE; *$p < 0.01$ and **$p < 0.001$ versus control cells. (C) Sensitized FRET analysis of RhoA activity in live CFBE41o-, CFBE41o-/sNHERF1, and CFBE41o-NHERF1-ΔERM cells. Cells were transfected with the RhoA FRET biosensor pRaichu-1297x, which shows a decrease in YFP emission upon GTP loading of RhoA, and then they were imaged for CFP and YFP emission. Activation of RhoA can be determined as an increase in the ratio of the CFP image over the YFP image. Data are the mean ± SE; ***$p < 0.0001$. (D) Pseudocolor images of representative CFBE41o-, CFBE41o-/sNHERF1, and CFBE41o-NHERF1-ΔERM cells in the FRET measurements of RhoA activity. FRET images, obtained as described in *Materials and Methods*, are presented in pseudocolor mode such that red indicates the highest EmCFP/EmYFP ratio (highest RhoA activity) and blue the lowest EmCFP/EmYFP ratio (lowest RhoA activity).

the NHERF1-dependent increase of phospho-ezrin in the membrane fraction of CFBE41o-/sNHERF1 cells (Figure 10A), 2) the increase of F-actin (Figure 10B), and 3) the rescue of CFTR activity (Figure 10C). Again the same pattern of inhibition of both F-actin content and CFTR-dependent chloride secretion induced by Y-27632 in CFBE41o-/sNHERF1 was also found in 16HBE14o- cells (Supplemental Figure 7S). Although we cannot exclude the possibility that other kinases besides ROCK could be affected by long Y-27632 preincubation, these data, altogether, suggest that there is a complex interaction network between these proteins and a possible positive feedback mechanism among NHERF1, RhoA, and ezrin that could further regulate F508del CFTR stability in the apical membrane by tethering it to the actin cytoskeleton.

DISCUSSION

NHERF1 was the first PDZ protein found to bind the C-terminal target domain of CFTR (Hall *et al*., 1998), and this interaction was demonstrated to regulate both CFTR polarized expression in the apical plasma membrane and the vectorial transport of chloride (Moyer *et al*., 2000). In this context, the association among the CFTR C terminus, NHERF1, ezrin, and the actin cytoskeleton has been proposed to physically tether CFTR on the membrane (Short *et al*., 1998). Indeed, NHERF1 has been found to be localized to the apical membrane in human airway 16HBE14o- cells expressing wt CFTR (Mohler *et al*., 1999; Guerra *et al*., 2005), whereas it is diffusely distributed in the cytoplasm in CFBE41o- (F508del/F508del) cells (Guerra *et al*., 2005). Moreover, in 16HBE14o- cell monolayers, wt NHERF1 overexpression increases, whereas NHERF1-ΔERM overexpression decreases both surface apical CFTR expression and activity (Guerra *et al*., 2005). Importantly, wt NHERF1 overexpression induces both a significant redistribution of NHERF1 and F508del CFTR from the cytoplasm to the apical membrane and rescues CFTR-dependent chloride secretion in polarized cell monolayers of CFBE41o- and CFT1-C2 cells (Guerra *et al*., 2005) as well as in Madin-Darby canine kidney (MDCK) monolayers transiently transfected with F508del CFTR (Bossard *et al*., 2007).

In this study, we have extended these findings and have analyzed the role of NHERF1 overexpression in influencing cytoskeletal organization, and, subsequently, the CFTR-dependent chloride efflux in both 16HBE14o- and CFBE41o- cells. Concerning 16HBE14o- polarized monolayers expressing wt CFTR, we found that they 1) displayed bundled actin filaments and treatment with the F-actin polymerization inhibitor cytochalasin D disorganized most of the actin filaments with a reduction of both F-actin content and CFTR-dependent chloride secretion; 2) NHERF1 overexpression increased both F-actin content, and as demonstrated previously (Guerra *et al*., 2005), CFTR activity, whereas NHERF1 knockdown inhibited these processes; 3) both cotransfection of wt NHERF1 with the FERM domain of ezrin, which blocks ezrin interaction with actin (Stanasila *et al*., 2006), or transfection of NHERF1 lacking its ezrin binding domain

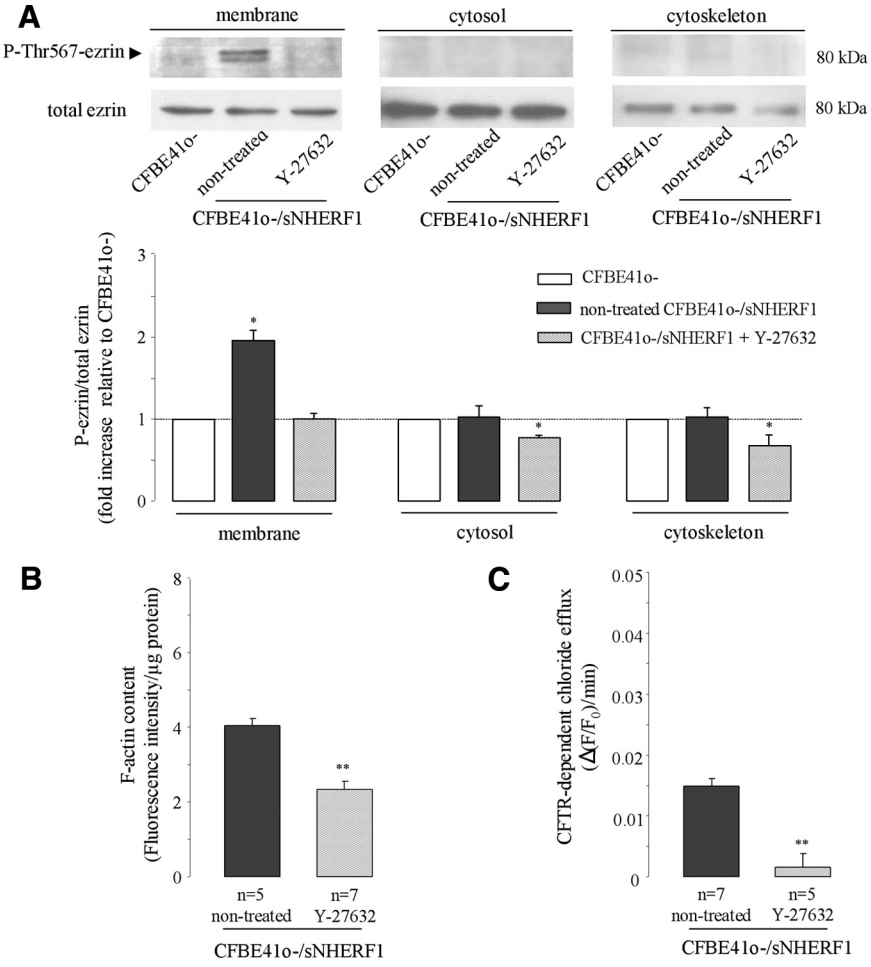

Figure 10. Involvement of ROCK signaling in ezrin phosphorylation, F-actin content, and CFTR-dependent chloride efflux. Cell fractionation analysis (A), F-actin content (B), and CFTR-dependent chloride efflux (C) were performed in control CFBE41o- cells and in CFBE41o-/sNHERF1 cells in control conditions and after 12-h treatment with the ROCK inhibitor Y-27632 (1 μM). (A) A representative Western blot analysis for phospho-ezrin at Thr567 (top band, arrowhead corresponding to the phosphorylated ezrin) and total ezrin in membrane, cytosolic and cytoskeletal fractions and the graphic representation of phospho-ezrin subcellular distribution expressed as the ratio of phospho-ezrin/total ezrin normalized in each fraction to that in nontreated CFBE41o- cells, designated as 1. Data are means ± SE, n = 5; *p < 0.01 versus nontreated CF cells. (B) Summary of F-actin content measurements expressed as described previously. Each bar represents the mean ± SE; **p < 0.001 versus nontreated cells. (C) Summary of CFTR-dependent chloride efflux calculated as described previously. Each bar represents the mean ± SE; **p < 0.001 versus nontreated monolayers.

(NHERF1-ΔERM) decreased both F-actin content and CFTR activity.

This correlation between the biochemical quantitative F-actin content and the functional measurements of CFTR activity together with the results of the coimmunoprecipitation experiments, favors the idea that in 16HBE14o- cells, NHERF1 is primarily involved in the regulation of the actin cytoskeleton network and the CFTR functional expression via the formation of the multiprotein complex CFTR-NHERF1-ezrin-actin. Our data are consistent with a growing body of evidence supporting the view that the organization of cytoskeleton network is strictly correlated with apical CFTR expression. It has been suggested that the cytoskeleton network can be a potential modulator of CFTR expression at the cell surface and proposed that actin disassembly, induced by neural Wiskott-Aldrich syndrome protein (N-WASP) inhibition, could attenuate CFTR confinement into a immobilized pool promoting its recruitment in clathrin coated pits as a prelude to its internalization (Ganeshan *et al*., 2007). Moreover, it has been demonstrated that although CFTR diffusion was highly confined under control conditions, it increased after C-terminal CFTR truncations, expression of NHERF1-ΔERM or by cytoskeletal disruption (Bates *et al*., 2006; Haggie *et al*., 2006). In line with the hypothesis that NHERF1 may stabilize wt CFTR on the apical membrane by linking it to the cytoskeleton, we found that NHERF1-ΔERM overexpression in 16HBE14o- monolayers increased CFTR internalization with respect to nontransfected cells (Figure 3).

In light of these results obtained in 16HBE14o- cells and the previous findings demonstrating that CFBE41o- cells express lower levels of NHERF1 than 16HBE14o- cells (Guerra *et al*., 2005), we hypothesized that the observed NHERF1 overexpression-dependent enhancement of the functional cell surface expression of F508del CFTR protein in CFBE41o- monolayers (Guerra *et al*., 2005), could be due, at least in part, to the effect of NHERF1 overexpression on actin cytoskeleton organization. Indeed, here we found that CFBE41o- polarized cells monolayers 1) displayed substantial disassembly of actin filaments; 2) overexpression of wt NHERF1, but not NHERF1-ΔERM, increased F-actin assembly, induced a small increase in cortical actin filaments, and rescued CFTR activity; 3) cotransfection of wt NHERF1 with ezrin-FERM blocked this NHERF1 overexpression-induced increase in both F-actin content and CFTR-dependent chloride secretion; 4) overexpressing wt NHERF1 greatly increased the interaction between CFTR, NHERF1, ezrin, and actin in coimmunoprecipitation experiments; and importantly, 5) the overexpression of wt NHERF1 in CFBE41o- cell monolayers decreased F508del CFTR internalization to levels of wt CFTR observed in 16HBE14o- cells (Figure 3). Altogether, these results demonstrate that wt NHERF1 overexpression in CFBE41o- cells, as we have found in 16HBE14o- cells, affects F-actin organization and assembly only when it can interact with ezrin.

Importantly, the phosphorylation of ezrin was necessary for the NHERF1-actin interaction because this interaction was compromised in CFBE41o-/sNHERF1 cells transfected with

the phospho-dead ezrin (ezrin T567A; Figure 5B). Indeed, ezrin activity is known to be regulated by intramolecular interactions between its N-(FERM) and C-terminal binding sites (Bretscher *et al*., 2002) and the phosphorylation of the C-terminal T567 residue maintains ezrin in the active state by suppressing this intramolecular interaction and thereby regulating its ability to interact with NHERF1 and actin (Matsui *et al*., 1998; Gautreau *et al*., 2000). It has been found that this active, open form of ezrin colocalizes with NHERF1 at or near the plasma membrane of polarized cells where they reciprocally stabilize each other and function together in organizing macromolecular complex (Morales *et al*., 2004). Indeed, here in confocal analysis performed in polarized monolayers phospho-ezrin was almost absent in nontransfected CFBE41o- cells, whereas it was relocalized beneath the apical membrane in CFBE41o- cell monolayers overexpressing wt NHERF1 (Figure 6A, bottom). Interestingly, a similar apical distribution of phospho-ezrin was found in 16HBE14o- monolayers (Figure 6B), suggesting that NHERF1 overexpression in CFBE41o- cells restores a "normal" phenotype. Furthermore, when we transfected CFBE41o- cells with the cDNA encoding the NHERF1-ΔERM construct, we found that the distribution of phospho-ezrin was similar to that found in nontransfected CFBE41o- cells. Similarly, the ratio of phosphorylated to total ezrin, determined in fractionation experiments, was much higher in the membrane fraction of CFBE41o-/sNHERF1 than in either nontransfected CFBE41o- cells or transfected with NHERF1-ΔERM (Figure 6A, top). Altogether, these data demonstrate that NHERF1 overexpression may regulate the phosphorylation of ezrin only when it can interact with N terminus of ezrin through its ERM binding domain. One possible hypothesis is that NHERF1 overexpression could displace the C terminus of ezrin for the binding with its N terminus, unmasking the F-actin binding site and, in this way, regulate the intramolecular association of ezrin and its subsequent activation and recruitment on the apical region. Furthermore, ezrin is a PKA-anchoring protein and when in its open form may recruit the regulatory subunit of PKA to the proximity of CFTR, leading to its activation (Sun *et al*., 2000).

Numerous studies have demonstrated that the small GTPase RhoA is a critical mediator of cytoskeletal organization (Tapon and Hall, 1997; Mackay and Hall, 1998) and regulates ERM protein phosphorylation (Matsui *et al*., 1999). Here, we show that the dominant-active mutant of RhoA, RhoA-V14, increases the amount of phospho-ezrin in the membrane fraction of CFBE41o- cells (Figure 7), causes an increase in the F-actin organization and assembly, rescues the CFTR-dependent chloride efflux, and induces a significant redistribution of F508del CFTR from the cytoplasm to the apical membrane (Figure 8 and Supplemental Figure 6S). These results confirm that RhoA activation is a crucial step for the ezrin phosphorylation, the organization of the actin cytoskeleton and the subsequent increase of F508del CFTR cell surface expression. Furthermore, the findings that RhoA-V14 did not cause a further increase in F-actin content or CFTR secretion in CFBE41o-/sNHERF1 as well as in 16HBE14o- cell monolayers suggests the hypothesis that the presence of NHERF1 in the multiprotein complex could be directly or indirectly involved in the activation of RhoA. This hypothesis is supported by the data demonstrating that RhoA activity is higher in both CFBE41o-/sNHERF1 and 16HBE14o- cells than in CFBE41o- cells transfected with NHERF1-ΔERM or in control CFBE41o- cells (Figure 9). Therefore, NHERF1, by interacting with ezrin, modulates ezrin activation that, in turn, may initiate the activation of RhoA. Indeed, the binding of Rho-GDP dissociation inhibitor (Rho-GDI) to the exposed N-terminal domain of ezrin has been demonstrated to release RhoA-GDP from the inhibitor, allowing its activation by a GDP-GTP exchange factor (Howard *et al*., 2000). Therefore, NHERF1-dependent recruitment of ezrin to the apical membrane of CFBE41o-/sNHERF1 cells not only would mediate its anchorage to the actin filaments but also would activate RhoA-dependent signaling. A similar signaling module has been described in MDCK cells where podocalyxin activates RhoA and induces actin reorganization through NHERF1 and ezrin (Schmieder *et al*., 2004). RhoA, once activated, may also contribute as a positive feedback to maintain ezrin in an active conformation via either ROCK-dependent phosphorylation of the C-terminal Thr567 residue in ezrin and/or by RhoA-dependent activation of phosphatidylinositol-4-phosphate 5-kinase, which controls the production of phosphatidylinositol 4,5-bisphosphate [PI(4,5)P2] (Bretscher *et al*., 2002; Yonemura *et al*., 2002; Ivetic and Ridley, 2004).

Depending on the cellular system analyzed, ROCK can play several roles in RhoA-induced actin organization and ROCK may either control actin filament bundling by regulating myosin light chain phosphorylation (Kimura *et al*., 1996) or promote F-actin accumulation by activating LIM kinases (Arber *et al*., 1998). The signaling pathways linking RhoA to F-actin assembly can also involve the diaphanous-related formins mDIA (Watanabe *et al*., 1997), and, in some cellular systems, mDIA and ROCK may cooperatively act as downstream targets of RhoA in Rho-induced changes in actin dynamics (Tominaga *et al*., 2000; Nakano *et al*., 2003). Here, we found that treatment with the selective ROCK inhibitor Y-27632 significantly decreased the amount of phospho-ezrin in the membrane fraction of CFBE41o-/sNHERF1 and inhibited the NHERF1 overexpression-dependent increase of F-actin assembly and CFTR-dependent chloride secretion in CFBE41o-/sNHERF1 cells. The dissection of the kinases down-stream of ROCK activation will be an important future field of research.

Altogether, these data provide further support for a central role of NHERF1 in regulating the formation of the ezrin-RhoA-ROCK-actin multiprotein complex and stabilizing both wt CFTR and F508del CFTR in the apical membrane. In CFBE41o/sNHERF1, we hypothesize (see model in Supplemental Figure 8S) that it is the overexpression of NHERF1 that regulates the formation of the CFTR-NHERF1-ezrin complex and that this complex, by activating the RhoA/ROCK pathway, increases F-actin organization and assembly and, in parallel, induces the phosphorylation of ezrin, which provides a regulated linkage between F508del CFTR and the actin cytoskeleton. This linkage stabilizes CFTR in the membrane by delaying its internalization and promoting the accumulation of F508del CFTR in the membrane. Further studies will be needed not only to define the exact sequence of events induced by NHERF1 overexpression in CFBE41o- cells that leads to RhoA activation but also the role of other eventual components of the multiprotein complex, such as PI(4,5)P2, that has been demonstrated to be required for the translocation of ERM proteins to the membrane (Yonemura *et al*., 2002; Fievet *et al*., 2004). Moreover, it will be important to analyze whether the different cellular localization of the components of the multiprotein complex identified in our heterologous cell systems occur in vivo; in this light, studies in wt, CF, or NHERF1 knockout mice will be valuable.

ACKNOWLEDGMENTS

We thank Prof. D. Gruenert for the kind gift the 16HBE14o- and CFBE41o cell lines. We also thank Dr. Susanna Cotecchia for helpful comments and advice on the manuscript. This work was supported by the Italian Cystic Fibrosis Research Foundation (grant FFC2/2007) with the contribution of the Christopher Ricardo Cystic Fibrosis Foundation, Loifur s.r.l., and Associazione Sergio Valente "100

alberi d'Autore," and by Deutsche Forschungsgemeinschaft grant SFB621-C9 and the German Mucoviscidosis Foundation e.V (to. U. S.).

REFERENCES

Arber, S., Barbayannis, F. A., Hanser, H., Schneider, C., Stanyon, C. A., Bernard, O., and Caroni, P. (1998). Regulation of actin dynamics through phosphorylation of cofilin by LIM-kinase. Nature *393*, 805–809.

Bates, I. R., Hebert, B., Luo, Y., Liao, J., Bachir, A. I., Kolin, D. L., Wiseman, P. W., and Hanrahan, J. W. (2006). Membrane lateral diffusion and capture of CFTR within transient confinement zones. Biophys. J. *91*, 1046–1058.

Benharouga, M., Sharma, M., So, J., Haardt, M., Drzymala, L., Popov, M., Schwapach, B., Grinstein, S., Du, K., and Lukacs, G. L. (2003). The role of the C terminus and Na+/H+ exchanger regulatory factor in the functional expression of cystic fibrosis transmembrane conductance regulator in nonpolarized cells and epithelia. J. Biol. Chem. *278*, 22079–22089.

Bossard, F., Robay, A., Toumaniantz, G., Dahimene, S., Becq, F., Merot, J., and Gauthier, C. (2007). NHE-RF1 protein rescues DeltaF508-CFTR function. Am. J. Physiol. Lung Cell Mol. Physiol. *292*, L1085–L1094.

Bradford, M. M. (1976). A rapid and sensitive method for the quantitation of microgram quantities of protein utilizing the principle of protein-dye binding. Anal. Biochem. *72*, 248–254.

Bretscher, A., Edwards, K., and Fehon, R. G. (2002). ERM proteins and Merlin: integrators at the cell cortex. Nat. Rev. Mol. Cell Biol. *3*, 586–599.

Bretscher, A., Reczek, D., and Berryman, M. (1997). Ezrin: a protein requiring conformational activation to link microfilaments to the plasma membrane in the assembly of cell surface structures. J. Cell Sci. *110*, 3011–3018.

Bronsveld, I., *et al*. (2000). Residual chloride secretion in intestinal tissue of deltaF508 homozygous twins and siblings with cystic fibrosis. The European CF Twin and Sibling Study Consortium. Gastroenterology *119*, 32–40.

Cardone, R. A., Bagorda, A., Bellizzi, A., Busco, G., Guerra, L., Paradiso, A., Casavola, V., Zaccolo, M., and Reshkin, S. J. (2005). Protein kinase A gating of a pseudopodial-located RhoA/ROCK/p38/NHE1 signal module regulates invasion in breast cancer cell lines. Mol. Biol. Cell *16*, 3117–3127.

Cheng, J., Moyer, B. D., Milewski, M., Loffing, J., Ikeda, M., Mickle, J. E., Cutting, G. R., Li, M., Stanton, B. A., and Guggino, W. B. (2002). A Golgi-associated PDZ domain protein modulates cystic fibrosis transmembrane regulator plasma membrane expression. J. Biol. Chem. *277*, 3520–3529.

Fievet, B. T., Gautreau, A., Roy, C., Del Maestro, L., Mangeat, P., Louvard, D., and Arpin, M. (2004). Phosphoinositide binding and phosphorylation act sequentially in the activation mechanism of ezrin. J. Cell Biol. *164*, 653–659.

Ganeshan, R., Nowotarski, K., Di, A., Nelson, D. J., and Kirk, K. L. (2007). CFTR surface expression and chloride currents are decreased by inhibitors of N-WASP and actin polymerization. Biochim. Biophys. Acta *1773*, 192–200.

Gautreau, A., Louvard, D., and Arpin, M. (2000). Morphogenic effects of ezrin require a phosphorylation-induced transition from oligomers to monomers at the plasma membrane. J. Cell Biol. *150*, 193–203.

Guerra, L., *et al*. (2005). Na+/H+ exchanger regulatory factor isoform 1 overexpression modulates cystic fibrosis transmembrane conductance regulator (CFTR) expression and activity in human airway 16HBE14o- cells and rescues DeltaF508 CFTR functional expression in cystic fibrosis cells. J. Biol. Chem. *280*, 40925–40933.

Guggino, W. B., and Stanton, B. A. (2006). New insights into cystic fibrosis: molecular switches that regulate CFTR. Nat. Rev. Mol. Cell Biol. *7*, 426–436.

Haggie, P. M., Kim, J. K., Lukacs, G. L., and Verkman, A. S. (2006). Tracking of quantum dot-labeled CFTR shows near immobilization by C-terminal PDZ interactions. Mol. Biol. Cell *17*, 4937–4945.

Haggie, P. M., Stanton, B. A., and Verkman, A. S. (2004). Increased diffusional mobility of CFTR at the plasma membrane after deletion of its C-terminal PDZ binding motif. J. Biol. Chem. *279*, 5494–5500.

Hall, R. A., Ostedgaard, L. S., Premont, R. T., Blitzer, J. T., Rahman, N., Welsh, M. J., and Lefkowitz, R. J. (1998). A C-terminal motif found in the beta2-adrenergic receptor, P2Y1 receptor and cystic fibrosis transmembrane conductance regulator determines binding to the Na+/H+ exchanger regulatory factor family of PDZ proteins. Proc. Natl. Acad. Sci. USA *95*, 8496–8501.

Hayashi, K., Yonemura, S., Matsui, T., and Tsukita, S. (1999). Immunofluorescence detection of ezrin/radixin/moesin (ERM) proteins with their carboxyl-terminal threonine phosphorylated in cultured cells and tissues. J. Cell Sci. *112*, 1149–1158.

Howard, M., Jiang, X., Stolz, D. B., Hill, W. G., Johnson, J. A., Watkins, S. C., Frizzell, R. A., Bruton, C. M., Robbins, P. D., and Weisz, O. A. (2000). Forskolin-induced apical membrane insertion of virally expressed, epitope-tagged CFTR in polarized MDCK cells. Am. J. Physiol. Cell Physiol. *279*, C375–C382.

Ivetic, A., and Ridley, A. J. (2004). Ezrin/radixin/moesin proteins and Rho GTPase signalling in leucocytes. Immunology *112*, 165–176.

Kalin, N., Claass, A., Sommer, M., Puchelle, E., and Tummler, B. (1999). DeltaF508 CFTR protein expression in tissues from patients with cystic fibrosis. J. Clin. Invest. *103*, 1379–1389.

Kimura, K., *et al*. (1996). Regulation of myosin phosphatase by Rho and Rho-associated kinase (Rho-kinase). Science *273*, 245–248.

Korichneva, I., and Hammerling, U. (1999). F-actin as a functional target for retro-retinoids: a potential role in anhydroretinol-triggered cell death. J. Cell Sci. *112*, 2521–2528.

Korichneva, I., Puceat, M., Cassoly, R., and Vassort, G. (1995). Cl^--$HCO3^-$ exchange in developing neonatal rat cardiac cells. Biochemical identification and immunolocalization of band 3-like proteins. Circ. Res. *77*, 556–564.

Kwon, S. H., Pollard, H., and Guggino, W. B. (2007). Knockdown of NHERF1 enhances degradation of temperature rescued DeltaF508 CFTR from the cell surface of human airway cells. Cell Physiol. Biochem. *20*, 763–772.

Li, C., and Naren, A. P. (2005). Macromolecular complexes of cystic fibrosis transmembrane conductance regulator and its interacting partners. Pharmacol. Ther. *108*, 208–223.

Lukacs, G. L., Chang, X., Bear, C., Kartner, N., Mohamed, A., Riordan, J. R., and Grinstein, S. (1993). The DF508 mutation decreases the stability of cystic fibrosis transmembrane conductance regulator in the plasma membrane. J. Biol. Chem. *268*, 21592–21598.

Ma, T., Thiagarajah, J. R., Yang, H., Sonawane, N. D., Folli, C., Galietta, L. J., and Verkman, A. S. (2002). Thiazolidinone CFTR inhibitor identified by high-throughput screening blocks cholera toxin-induced intestinal fluid secretion. J. Clin. Invest. *110*, 1651–1658.

Mackay, D. J., and Hall, A. (1998). Rho GTPases. J. Biol. Chem. *273*, 20685–20688.

Matsui, T., Maeda, M., Doi, Y., Yonemura, S., Amano, M., Kaibuchi, K., and Tsukita, S. (1998). Rho-kinase phosphorylates COOH-terminal threonines of ezrin/radixin/moesin (ERM) proteins and regulates their head-to-tail association. J. Cell Biol. *140*, 647–657.

Matsui, T., Yonemura, S., and Tsukita, S. (1999). Activation of ERM proteins in vivo by Rho involves phosphatidyl-inositol 4-phosphate 5-kinase and not ROCK kinases. Curr. Biol. *9*, 1259–1262.

Mohler, P. J., Kreda, S. M., Boucher, R. C., Sudol, M., Stutts, M. J., and Milgram, S. L. (1999). Yes-associated protein 65 localizes p62(c-Yes) to the apical compartment of airway epithelia by association with EBP50. J. Cell Biol. *147*, 879–890.

Morales, F. C., Takahashi, Y., Kreimann, E. L., and Georgescu, M. M. (2004). Ezrin-radixin-moesin (ERM)-binding phosphoprotein 50 organizes ERM proteins at the apical membrane of polarized epithelia. Proc. Natl. Acad. Sci. USA *101*, 17705–17710.

Moyer, B. D., *et al*. (1999). A PDZ-interacting domain in CFTR is an apical membrane polarization signal. J. Clin. Invest. *104*, 1353–1361.

Moyer, B. D., *et al*. (2000). The PDZ-interacting domain of cystic fibrosis transmembrane conductance regulator is required for functional expression in the apical membrane. J. Biol. Chem. *275*, 27069–27074.

Nakano, M., Okamoto, Y., Ohzeki, J., and Masumoto, H. (2003). Epigenetic assembly of centromeric chromatin at ectopic alpha-satellite sites on human chromosomes. J. Cell Sci. *116*, 4021–4034.

Okiyoneda, T., and Lukacs, G. L. (2007). Cell surface dynamics of CFTR: the ins and outs. Biochim. Biophys. Acta *1773*, 476–479.

Paradiso, A., Cardone, R. A., Bellizzi, A., Bagorda, A., Guerra, L., Tommasino, M., Casavola, V., and Reshkin, S. J. (2004). The Na+-H+ exchanger-1 induces cytoskeletal changes involving reciprocal RhoA and Rac1 signaling, resulting in motility and invasion in MDA-MB-435 cells. Breast Cancer Res. *6*, R616–R628.

Prat, A. G., Xiao, Y. F., Ausiello, D. A., and Cantiello, H. F. (1995). cAMP-independent regulation of CFTR by the actin cytoskeleton. Am. J. Physiol. *268*, C1552–C1561.

Raghuram, V., Mak, D. D., and Foskett, J. K. (2001). Regulation of cystic fibrosis transmembrane conductance regulator single-channel gating by bivalent PDZ-domain-mediated interaction. Proc. Natl. Acad. Sci. USA *98*, 1300–1305.

Schmieder, S., Nagai, M., Orlando, R. A., Takeda, T., and Farquhar, M. G. (2004). Podocalyxin activates RhoA and induces actin reorganization through NHERF1 and Ezrin in MDCK cells. J. Am. Soc. Nephrol. *15*, 2289–2298.

Sharma, M., Benharouga, M., Hu, W., and Lukacs, G. L. (2001). Conformational and temperature-sensitive stability defects of the delta F508 cystic fibrosis transmembrane conductance regulator in post-endoplasmic reticulum compartments. J. Biol. Chem. *276*, 8942–8950.

Sheppard, D. N., and Welsh, M. J. (1999). Structure and function of the CFTR chloride channel. Physiol. Rev. *79*, S23–S45.

Short, D. B., Trotter, K. W., Reczek, D., Kreda, S. M., Bretscher, A., Boucher, R. C., Stutts, M. J., and Milgram, S. L. (1998). An apical PDZ protein anchors the cystic fibrosis transmembrane conductance regulator to the cytoskeleton. J. Biol. Chem. *273*, 19797–19801.

Silvis, M. R., Bertrand, C. A., Ameen, N., Golin-Bisello, F., Butterworth, M. B., Frizzell, R. A., and Bradbury, N. A. (2009). Rab11b regulates the apical recycling of the cystic fibrosis transmembrane conductance regulator in polarized intestinal epithelial cells. Mol. Biol. Cell *20*, 2337–2350.

Stanasila, L., Abuin, L., Diviani, D., and Cotecchia, S. (2006). Ezrin directly interacts with the alpha1b-adrenergic receptor and plays a role in receptor recycling. J. Biol. Chem. *281*, 4354–4363.

Sun, F., Hug, M. J., Bradbury, N. A., and Frizzell, R. A. (2000). Protein kinase A associates with cystic fibrosis transmembrane conductance regulator via an interaction with ezrin. J. Biol. Chem. *275*, 14360–14366.

Swiatecka-Urban, A., *et al*. (2005). The short apical membrane half-life of rescued {Delta}F508-cystic fibrosis transmembrane conductance regulator (CFTR) results from accelerated endocytosis of {Delta}F508-CFTR in polarized human airway epithelial cells. J. Biol. Chem. *280*, 36762–36772.

Swiatecka-Urban, A., Duhaime, M., Coutermarsh, B., Karlson, K. H., Collawn, J., Milewski, M., Cutting, G. R., Guggino, W. B., Langford, G., and Stanton, B. A. (2002). PDZ domain interaction controls the endocytic recycling of the cystic fibrosis transmembrane conductance regulator. J. Biol. Chem. *277*, 40099–40105.

Taddei, A., Folli, C., Zegarra-Moran, O., Fanen, P., Verkman, A. S., and Galietta, L. J. (2004). Altered channel gating mechanism for CFTR inhibition by a high-affinity thiazolidinone blocker. FEBS Lett. *558*, 52–56.

Tapon, N., and Hall, A. (1997). Rho, Rac and Cdc42 GTPases regulate the organization of the actin cytoskeleton. Curr. Opin. Cell Biol. *9*, 86–92.

Tominaga, T., Sahai, E., Chardin, P., McCormick, F., Courtneidge, S. A., and Alberts, A. S. (2000). Diaphanous-related formins bridge Rho GTPase and Src tyrosine kinase signaling. Mol. Cell *5*, 13–25.

Uehata, M., Ishizaki, T., Satoh, H., Ono, T., Kawahara, T., Morishita, T., Tamakawa, H., Yamagami, K., Inui, J., Maekawa, M., and Narumiya, S. (1997). Calcium sensitization of smooth muscle mediated by a Rho-associated protein kinase in hypertension. Nature *389*, 990–994.

Wang, S., Yue, H., Derin, R. B., Guggino, W. B., and Li, M. (2000). Accessory protein facilitated CFTR-CFTR interaction, a molecular mechanism to potentiate the chloride channel activity. Cell *103*, 169–179.

Watanabe, N., Madaule, P., Reid, T., Ishizaki, T., Watanabe, G., Kakizuka, A., Saito, Y., Nakao, K., Jockusch, B. M., and Narumiya, S. (1997). p140mDia, a mammalian homolog of Drosophila diaphanous, is a target protein for Rho small GTPase and is a ligand for profilin. EMBO J. *16*, 3044–3056.

Yonemura, S., Matsui, T., and Tsukita, S. (2002). Rho-dependent and -independent activation mechanisms of ezrin/radixin/moesin proteins: an essential role for polyphosphoinositides in vivo. J. Cell Sci. *115*, 2569–2580.

Yoshizaki, H., Ohba, Y., Parrini, M. C., Dulyaninova, N. G., Bresnick, A. R., Mochizuki, N., and Matsuda, M. (2004). Cell type-specific regulation of RhoA activity during cytokinesis. J. Biol. Chem. *279*, 44756–44762.